INTERNATIONAL JOURNAL OF CLIMATOLOGY
Int. J. Climatol. **37** (Suppl.1): 1035–1052 (2017)
Published online 4 April 2017 in Wiley Online Library
(wileyonlinelibrary.com) DOI: 10.1002/joc.5056

RMetS
Royal Meteorological Society

A climatological validation of urban air temperature and electricity demand simulated by a regional climate model coupled with an urban canopy model and a building energy model in an Asian megacity

Yuya Takane,[a]* Yukihiro Kikegawa,[b] Masayuki Hara,[c] Tomohiko Ihara,[d] Yukitaka Ohashi,[e] Sachiho A. Adachi,[f] Hiroaki Kondo,[a] Kazuki Yamaguchi[g] and Naoki Kaneyasu[a]

[a] *Environmental Management Research Institute, National Institute of Advanced Industrial Science and Technology, Tsukuba, Japan*
[b] *School of Science and Engineering, Meisei University, Tokyo, Japan*
[c] *Center for Environmental Science in Saitama, Kazo, Japan*
[d] *Graduate School of Frontier Science, The University of Tokyo, Kashiwa, Japan*
[e] *Faculty of Biosphere–Geosphere Science, Okayama University of Science, Okayama, Japan*
[f] *RIKEN Advanced Institute for Computational Science, Kobe, Japan*
[g] *TEPCO Research Institute, Tokyo Electric Power Company Holdings, Inc, Yokohama, Japan*

ABSTRACT: In this study, we validated urban air temperature and electricity demand by a year-round numerical simulation using a regional climate model coupled with an urban canopy model and a building energy model (RCM-UCM+BEM) in the Asian megacity, Osaka, which is the largest metropolis in Japan after Tokyo. The control simulation (CTRL), which was based on the use of central air-conditioning (AC) systems, reproduced the surface air temperatures observed in Osaka City in the summer cooling and interim seasons, but underestimated midnight to morning temperatures by over 2 °C in the winter heating season. In addition, the CTRL significantly overestimated the electricity demand in Osaka City in both the cooling and heating seasons, when the AC load was increased. These errors were likely due to the overestimation of AC use in the CTRL model because, in Japan, central AC systems are not used in business and residential areas, where individual AC units are mainly used. To prevent this overestimation, we introduced three new parameters to consider the use of partial AC systems in the model. The results of the new numerical experiment remarkably reduced the underestimation of temperature and the overestimation of electricity demand. This suggests that the RCM-UCM+BEM modified by this study is effective for not only reproducing the current status of seasonal urban air temperature and electricity demand in Osaka, but also for projecting the future situation in other mega cities.

KEY WORDS urban climate; electricity demand; building energy model; regional climate model; mega city

Received 18 May 2016; Revised 6 February 2017; Accepted 11 February 2017

1. Introduction

In 2014, 54% of the entire world's population lived in metropolitan areas, with the percentage projected to increase to 66% by 2050 (United Nations, Department of Economic and Social Affairs, Population Division, 2014). In particular, the United Nations, Department of Economic and Social Affairs, Population Division (2014) showed that the population living in Asian urban areas would increase substantially. The concentration of population in urban areas causes several social problems, such as food and water supply issues, heat stroke, air pollution and increased energy demand, as well as environmental impacts. It is likely that these problems will be exacerbated by climate change (e.g. IPCC, 2014), without carefully planning the spatial arrangement of cities. An increase in energy demand in urban areas is one of the biggest social issues associated with urbanization. In particular, energy demand will dramatically increase in developing countries (Ministry of Economy, Trade and Industry of Japan, 2015) due to population increases, urban development, and climate change.

In general, energy demand, including the use of air-conditioning (AC) systems, is strongly related to the urban climate, which is affected by the urban heat island effect (local phenomenon) and climate change (global phenomenon). When the urban temperature rises due to the heat island effect and climate change, energy demand is also increased due to the greater use of AC systems. This process causes an increase in anthropogenic heat release from indoor to outdoor locations in summertime. The released anthropogenic heat enhances the heat island effect. This positive feedback process has been

* Correspondence to: Y. Takane, Environmental Management Research Institute, National Institute of Advanced Industrial Science and Technology, 16-1 Onogawa, Tsukuba, Ibaraki 305-8569, Japan. E-mail: takane.yuya@aist.go.jp

described in previous reports (e.g. Ashie *et al.,* 1999; Kikegawa *et al.,* 2003, 2014; Sailor, 2011).

Numerical simulations are effective means of evaluating this relationship between urban climate and energy demand in an urban area. In the 1990s, many studies used urban slab parameterization in a limited area model to reproduce fundamental meteorological elements, such as temperature, humidity, and wind components in urban areas (e.g. Seaman *et al.,* 1989; Kimura and Takahashi, 1991; Ichinose *et al.,* 1999; Kanda *et al.,* 2001). After the late 1990s, urban canopy models (UCMs) coupled with limited area models/regional climate models (RCMs), which more realistically take into account many physical processes in urban areas, were developed (e.g. Kondo and Liu, 1998; Masson, 2000; Kusaka *et al.,* 2001; Martilli *et al.,* 2002; Kanda *et al.,* 2005). Other researchers also developed UCMs, and studied urban environments using these models. Grimmond *et al.* (2010, 2011) and Best and Grimmond (2015) compared these UCMs and summarized their features. The UCMs can take into consideration anthropogenic heat due to human activities, including the use of AC and traffic. Generally, this anthropogenic heat is treated as a static value in the source term of surface energy budget equations. A single-layer UCM developed by Kusaka *et al.* (2001) and Kusaka and Kimura (2004a, 2004b) was coupled with the Weather Research and Forecasting (WRF) model (Skamarock *et al.,* 2008) (hereafter WRF-SLUCM), and has been widely used in many case studies (e.g. Takane and Kusaka, 2011; Takane *et al.,* 2013, 2015b) and climate simulations in urban areas (e.g. Kusaka *et al.,* 2012a; Adachi *et al.,* 2014).

In the early 2000s, a simple building energy model (BEM), which can dynamically calculate energy demand and anthropogenic heat due to the use of AC, was developed by Kikegawa *et al.* (2003), and coupled with a multi-layer UCM (CM-BEM) developed by Kondo and Liu (1998) and Kondo *et al.* (2005) for weather and climate simulation. This coupled model has been used in several urban climate and energy demand studies (e.g. Kondo and Kikegawa, 2003; Kikegawa *et al.,* 2006; Tokairin *et al.,* 2006; Ohashi *et al.,* 2007; Ihara *et al.,* 2008). Kikegawa *et al.* (2014) combined the CM-BEM with the WRF model (hereafter WRF-CM-BEM). It has been used to evaluate urban climate, energy demand, the effects of heat island countermeasures and health impacts (Ohashi *et al.,* 2014, 2016a; Takane *et al.,* 2015a). Salamanca and Martilli (2010), Salamanca *et al.* (2010) and Bueno *et al.* (2012) also developed BEMs, and combined them with a building effect parameterization (BEP) model (Martilli *et al.,* 2002) in the WRF model (hereafter WRF-BEP+BEM) and town energy budget (TEB) model (Masson, 2000) (hereafter BEM+TEB), respectively. In general, these are simplifications of detailed BEMs, such as EnergyPlus (Crawley *et al.,* 2001), which is mainly used in the field of architecture. Thus, these simplified BEMs can reduce computational cost and are currently suitable for real weather and climate studies in urban areas at the city block scale.

The WRF-SLUCM has been validated by many previous studies (e.g. Kusaka *et al.,* 2010, 2012a), and has been used not only for past climate simulations, but also future climate projections (e.g. Kusaka *et al.,* 2012b; Lemonsu *et al.,* 2013; Kikumoto *et al.,* 2016), as well as for urban planning strategies (e.g. Adachi *et al.,* 2014; Iizuka *et al.,* 2015; Yang *et al.,* 2016). On the other hand, WRF-CM-BEM and WRF-BEP+BEM have yet to be sufficiently and climatologically evaluated, and have been used infrequently in future climate projections. Kikegawa *et al.* (2014) validated the urban temperature and energy demand simulated by WRF-CM-BEM in Greater Tokyo during four consecutive clear-sky summer weekdays. They demonstrated that the model successfully reproduced the daily variation of the urban temperature and the actual areal electricity demand in the city's business area, but overestimated the demand in the residential area. Salamanca *et al.* (2010) investigated the reproducibility of total cooling energy simulated by WRF-BEP+BEM in a Tokyo office area over several days, and compared the results with those simulated by the WRF-CM-BEM. Another validation of BEP+BEM was conducted by Salamanca *et al.* (2013). In that validation, the authors directly compared electricity demand simulated by WRF-BEP+BEM with the actual AC consumption provided by the local electricity utility company during several summer extreme heat events over the rapidly urbanising semi-arid region of the Phoenix metropolitan area in the United States. They showed that WRF-BEP+BEM was able to satisfactorily reproduce the observed diurnal profile of AC electricity consumption in Phoenix. Bueno *et al.* (2011) coupled the detailed BEM EnergyPlus with TEB (hereafter EnergyPlus-TEB). They evaluated the reproducibility of air temperature and electricity demand simulated by this model using measurements conducted by CAPITOUL (Masson *et al.,* 2008) over the dense urban centre of Toulouse, France, during summer and winter. Bueno *et al.* (2012) showed that the BEM-TEB was able to reproduce the results of a more sophisticated BEM, such as EnergyPlus. They also compared the model results with the CAPITOUL data and found reasonable agreement. However, in previous studies, the validation periods have been relatively short (e.g. several days or a few months), and the spatial distribution and total real electricity demand in the entire urban area was not assessed. A relatively long-term (e.g. year-round) and more detailed validation, including the reproducibility of spatial distribution and total electricity demand, are essential to accurately project and assess the effects of urban development and climate change, especially in developing cities in Asia.

In general, summertime air temperature is high in many Asian countries. In Southeast Asia, it is hot all year-round and humid in summer, because of the low-latitude location in the proximity to the sea. It is expected that energy demand due to the use of AC systems will increase rapidly when they become widely available in these countries with the progression of global climate change and the heat island effect. Urban climate and energy demand projections with urbanization and climate change are scientifically and socially important for the evaluation of uncertainties over future urban climate. However, a

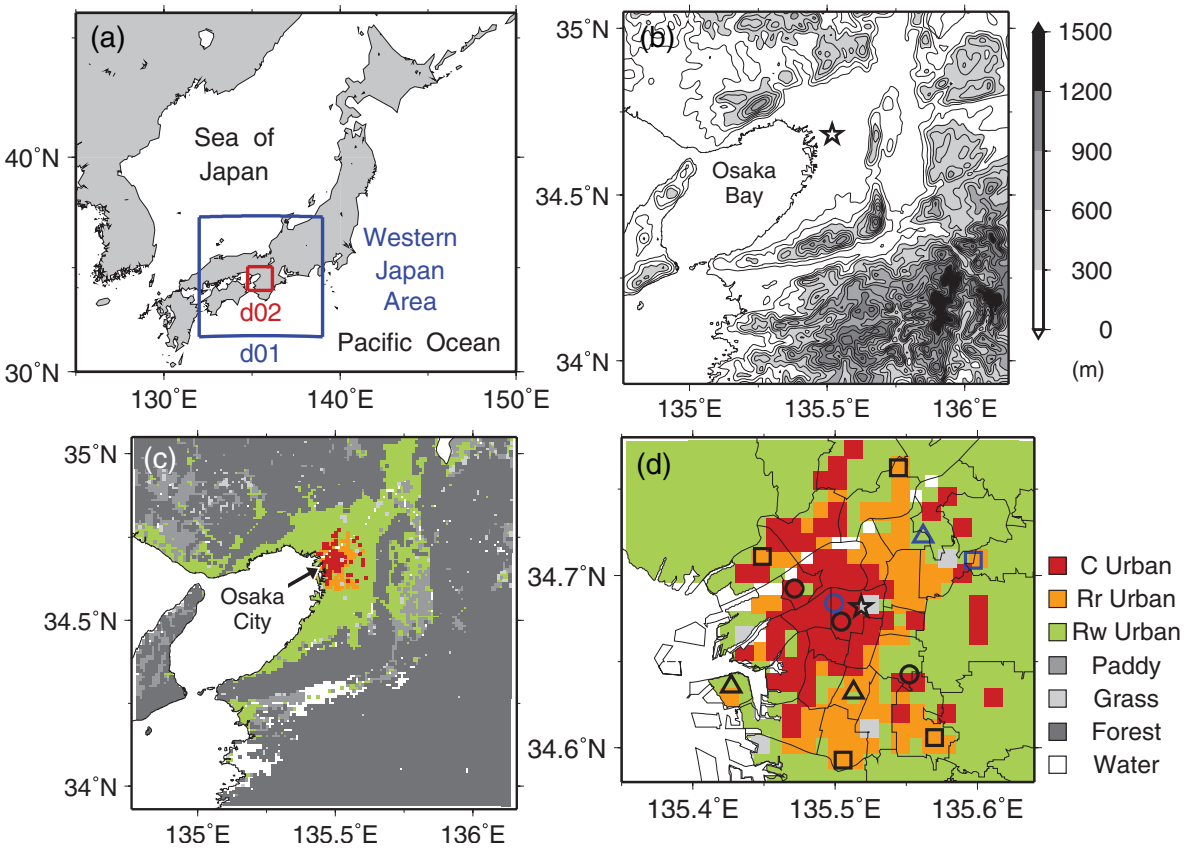

Figure 1. The study area. (a) Map of Japan, (b) topography, (c) and (d) land-use categories over the Osaka Plain area (the domain of the numerical simulations), and Osaka City, with the locations of the observation sites. The star is the Osaka Automated Meteorological Data Acquisition System (AMeDAS) site. The circles, squares, and triangles in (d) show observation sites for urban categories, including commercial and office buildings (C), fireproof apartments (Rr), and wooden detached dwelling (Rw), respectively. The blue circles, squares, and triangles are reference observation sites for each urban category for validation.

thorough validation of the RCM coupled with the UCM and BEM has to be performed before it is used for an actual projection.

In this study, we validated the urban air temperature and energy demand by a year-round numerical simulation using the RCM coupled with the UCM and the BEM in the Asian megacity Osaka (Figure 1), which is the largest metropolis in Japan after Tokyo. The city has a population of about 2.66 million, and has experienced the highest summertime average temperatures in Japan over the past 30 years (1981–2010). In this validation, we investigated the diurnal variation, horizontal distribution, and total energy demand in the urban area in Osaka. The results will help to project future urban climate and energy demands in other Asian mega cities. They will also be applicable to projections in high-latitude cities in Europe and North America in future situations where AC systems are widely used.

2. Description of the numerical simulation and the data used

2.1. Description of the numerical simulation

We used the Advanced Research WRF model (ver. 3.5.1) (Skamarock *et al.,* 2008). The model domain shown in Figure 1(a) covers the area of western Japan, including Osaka City, which was the focus of our study. Both the d01 and d02 domains consisted of 126 grid points in the x and y directions. We set the horizontal grid spacing to 5 and 1 km in domains 1 and 2, respectively. The model top was 50 hPa, with 35 vertical sigma levels. In this simulation, the initial and boundary conditions were derived from the National Centers for Environmental Prediction-National Center for Atmospheric Research (NCEP–NCAR) reanalysis data (Kalnay *et al.,* 1996) and merged satellite and *in situ* data global daily (MGD) sea surface temperature (SST) data (Kurihara *et al.,* 2006). The simulation period was from April 2013 to March 2014, but time integration was conducted continually from 5 days before the start of each month to the end of the month. For example, in August, time integration was conducted from 0000 UTC 27 July to 1 September.

The following schemes were used in the simulation: the updated Rapid Radiation Transfer Model (RRTMG) short-wave and long-wave radiation schemes (Iacono *et al.,* 2008); the WRF single-moment three-class (WSM3) cloud microphysics scheme (Dudhia, 1989; Hong *et al.,* 2004); the Mellor–Yamada–Janjic (MYJ) atmospheric boundary-layer scheme (Mellor and Yamada, 1982; Janjic, 1994, 2002); the Noah land surface model (Chen and

Dudhia, 2001); and the BEP+BEM model (Martilli *et al.,* 2002; Salamanca and Martilli, 2010; Salamanca *et al.,* 2010).

2.2. Description of the UCM and BEM

The BEP+BEM was selected as the BEM because, compared to the other BEMs currently in use, the BEP+BEM is officially coupled with the WRF model and has greater potential to be widely used worldwide. Here, we describe some features of the BEP+BEM that were not described in detail by Salamanca and Martilli (2010) and Salamanca *et al.* (2010, 2013, 2014): (1) the BEP+BEM assumes a central AC system and does not allow for partial AC, which means that the BEP+BEM cannot distinguish between separate rooms with and without individual AC units; (2) the BEP+BEM does not take into account anthropogenic heat due to traffic; (3) the BEP+BEM cannot calculate variation in the coefficient of performance (COP) of a heat pump variation over time, which means that COP is a constant value in this model; and (4) the model can only deal with the weekday situation, as described above.

2.3. Anthropogenic heat calculation

In this study, we calculated the anthropogenic heat due to the use of AC during the cooling season (Kikegawa *et al.,* 2003) in every time step as:

$$Q_{\mathrm{A}} = \left(H_{\mathrm{out}} + E_{\mathrm{out}}\right) + E_c = \frac{\mathrm{COP}+1}{\mathrm{COP}}\left(H_{\mathrm{out}} + E_{\mathrm{out}}\right) \tag{1a}$$

Here, Q_{A} denotes the total anthropogenic heat due to the use of AC, E_{c} indicates the electricity demand, and H_{out} and E_{out} indicate the sensible and latent heat supplied from the system for room cooling, respectively. In this study, we divided Q_{A} into sensible heat, Q_{AS}, and latent heat, Q_{AL}, referring to the results of Shimoda *et al.* (2002) as follows:

$$Q_{\mathrm{AS}} = 0.722 Q_{\mathrm{A}} \tag{1b}$$

$$Q_{\mathrm{AL}} = 0.278 Q_{\mathrm{A}} \tag{1c}$$

Shimoda *et al.* (2002) investigated the actual use of AC, including electric and gas systems, in Osaka, and reported the ratio between Q_{AS} and Q_{AL} by an inventory approach.

The anthropogenic heat due to the use of AC during the heating season was calculated as follows:

$$Q_{\mathrm{AS}} = H_{\mathrm{out}} - E_{\mathrm{c}} = \frac{\mathrm{COP}-1}{\mathrm{COP}} H_{\mathrm{out}} \tag{2}$$

Here, for a heat pump with a natural source of air, Q_{AL} is set to 0.

Krpo *et al.* (2010) reported the impact of anthropogenic heat due to use of AC on the boundary layer using the WRF-BEP+BEM. Although they used the right-hand side of Equation (1a) to calculate Q_{AS} in their simulation, in our study, we use it to calculate Q_{A}, which includes both Q_{AS} and Q_{AL}, as E_{out} was already considered. Moreover, although they defined $Q_{\mathrm{AL}} = E_{\mathrm{out}}$ using Equation (1b) in their study, this does not reflect the real situation because the latent heat load in a building is released directly outside rather than through the system in this setting. Furthermore, it is possible that Q_{AL} was doubly counted in their study because it was already considered in their Equation (1a), as described above. Therefore, we used the more realistic Equations (1a) and (2), as with WRF-CM-BEM. In this study, we refer to this simulation as the CTRL case.

2.4. Data required for the numerical simulation and validation

The model used in this study required identification of more parameters for detailed building energy budget calculations. For the geometric parameters of urban canopies, the mean building width, mean distance between buildings, and distribution of building height had to be set in each urban category. These settings were derived from the same building polygon data. For the building energy simulation, the typical materials and physical properties of walls and roofs were set based on the values in the literature for the three building prototypes. These settings are shown in Table 1, with the configurations of AC systems installed in each building prototype used in the simulations determined by reference to previous studies (e.g. Ihara *et al.,* 2008; Kikegawa *et al.,* 2014; Takane *et al.,* 2015a).

In Osaka, actual energy demand data are available with high spatial and temporal resolution. Specifically, the data were hourly electricity consumption data over Osaka City recorded in kilowatt-hour units. The data were divided into distinct urban areas, delineated based on the area supplied by electric power by individual substations. As with Ohashi *et al.* (2016b), polygon data from the geographical information system (GIS) in Osaka City were used to identify the building utilization within the delineated areas. These data included the building use and total floor area for each building in Osaka. The main building types in the 12 districts were analysed based on the most occupied building type within the area supplied with electric power by a particular substation. We also used the Automated Meteorological Data Acquisition System (AMeDAS) data provided by the Japan Meteorological Agency.

Figure 2 shows the relationship between seasonal variation in total daily electricity demand in the 12 districts around Osaka City and the average daily temperature observed at a height of 1.5 m at the Osaka AMeDAS station (Figures 1(b) and (d)) from April 2013 to March 2014. The daily averaged temperature increased from April 2013 due to seasonal variation, and peaked on August 2013. After August, the temperature gradually decreased to February 2014. The daily electricity demand also increased from April to August 2013. In particular, the electricity demand increased significantly from early July 2013, which indicated that many people began to use AC for cooling rooms and/or floors from this time onwards. After August, both the electricity demand and the temperature decreased to the end of October 2013. Electricity demand increased again from early November 2013 to February 2014, due to the use of AC for heating. In this study, we defined July to September 2013 as the cooling season, and November

Table 1. Parameter settings for the WRF-BEP+BEM model. The parameters were obtained from the Energy Conservation Center of Japan (2005), Kikegawa *et al.* (2006, 2014), and Takane *et al.* (2015a).

Urban categories		Material	Thermal conductivity (W m^{-1} K^{-1})	Volumetric heat capacity (× 10^6 J m^{-3} K^{-1})	Surface albedo (−)	Surface emissivity (−)
Commercial (C)	Roof (Thickness 0.03 m/layer, Total: 0.3 m (10 layers))	Lightweight concrete/concrete/rock-wool board (except 3-4th layers)	0.520	1.4650	0.20	0.97
		Insulation (air gap/styrene foam) (3-4th layer)	0.014	0.09346	–	–
	Wall (0.0225 m/layer, Total: 0.225 m (10 layers))	Tile/mortar/concrete/sealed air gap/plasterboard (except 9th layer)	0.710	1.6950	0.20	0.97
		Insulation (air gap/styrene foam) (9th layer)	0.019	0.06675	–	–
		Window (glass)	- Area fraction on the walls: 0.33			
	AC system	Electric air-source heat-pumps (rated COP = 3.58 (cooling) 3.64 (heating)): 100% - Target room temperature 27 °C (cooling) and 22 °C (heating) - Air-conditioning period: June 1st – September 30th (cooling), and November 1st – March 31st (heating) - Initial and end local times of AC system:8-19 (LT)				
	Heat generated by equipment	- Peak value: 21.23 (W m^{-2}) - Diumal variation (ratio of several times values to peak value): 0.31, 0.29, 0.29, 0.28, 0.29, 0.31, 0.40, 0.50, 0.74, 0.91, 0.95, 0.98, 0.99, 1.00, 0.98, 0.97, 0.95, 0.92, 0.79, 0.70, 0.59, 0.50, 0.43 and 0.36 from 0 to 23 JST (UTC+9h)				
Fire-proof apartment (Rr)	Roof (0.0225 m/layer, Total: 0.225 m (10 layers))	Concrete/styrene foam/asphalt (except 3rd layer)	0.897	1.8150	0.20	0.97
		Insulation (air gap/styrene foam) (3rd layer)	0.030	0.04376	–	–
	Wall (0.0234 m/layer, Total: 0.234 m (10 layers))	Concrete/plasterboard (except 9th layer)	1.050	1.9340	0.20	0.97
		Insulation (air gap/styrene foam) (9th layer)	0.042	0.03126	–	–
		Window (glass)	- Area fraction on the walls: 0.18			
	AC system	Electric air-source packaged air conditioners (rated COP = 5.03): 1.00% - Target room temperature : 28 °C (cooling) and 20 °C (heating) - Air-conditioning period: 1 June −30 September (cooling), and 1 November−31 March (heating) - Initial and end local times of AC system: 0−24 (LT)				
	Heat generated by equipment	- Peak value: 5.2 (W m^{-2}) - Diumal variation (ratio of several times values to peak value): 0.31, 0.29, 0.29, 0.28, 0..29, 0.31, 0.40, 0.50, 0.74, 0.91, 0.95, 0.98, 0.99, 1.00, 0.98, 0.97, 0.95, 0.92, 0.79, 0.59, 0.50, 0.43 and 0.36 from 0 to 23 JST (UTC+9h)				
Wooden detached dwellings (Rw)	Roof (0.0095 m/layer, Total: 0.095 m (10 layers))	Slate/plywood/plasterboard (except 5-8th layers)	0.181	0.5281	0.20	0.97
		Insulation (air gap/styrene foam) (5-8th layer)	0.032	0.02616		
	Wall (0.011 m/layer, Total: 0.11 m (10 layers))	Mortar/plywood/plasterboard (except 5-8th layers)	0.323	0.9983	0.20	0.97
		Insulation (air gap/styrene foam) (5-8th layer)	0.032	0.02616		
		Window (glass)	- Area fraction on the walls: 0.18			
	AC system	Electric air-source packground air conditioners (rated COP = 5.03): 100% - Target room temperature : 28 °C (cooling) and 20 °C (heating) - Air-conditioning period: 1 June−30 September (cooling), and 1 November−31 March (heating) - Initial and end local times of AC system 0−24 (LT)				
	Heat generated by equipment	- Peak value: 5.2 (W m^{-2}) - Diumal variation (ratio of several times values to peak value): 0.31, 0.29, 0.29, 0.28, 0.29, 0.31, 0.40, 0.50, 0.74, 0.91, 0.95, 0.98, 099, 1.00, 0.98, 0.97, 0.95, 0.92, 0.79, 0.70, 0.59, 0.50, 0.43 and 0.36 from 0 to 23 JST (UTC+9h)				

Int. J. Climatol. **37** (Suppl.1): 1035–1052 (2017)

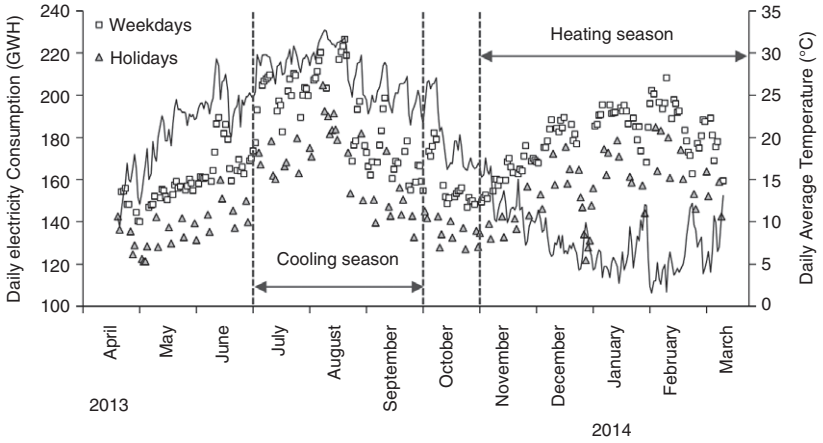

Figure 2. Seasonal variation in the sum of the daily electricity demand in all of Osaka City including the 12 districts (marks), and daily average temperature observed at 1.5-m height at the AMeDAS site (solid line). Squares and triangles indicate the electricity demand on weekdays and weekends, including holidays, respectively. This figure is a modification of Figure 2 in Ohashi *et al.* (2016b).

2013 to March 2014 as the heating season, in reference to the above features of temperature and electricity demand. The periods from April to June and October 2013 were defined as the interim seasons.

Note that we only used weekday electricity demand data for validation, because the numerical model used in this study only considered the weekday situation. In this study, we use the weekday base load data (the constant part of the total load not including electricity demand due to use of AC) estimated by Hashimoto *et al.* (2016). These base loads, with 1-h resolution, were estimated for all of the substations shown in Figure 1(d).

The land use and land cover (LULC) and topographic datasets of the Geospatial Information Authority of Japan (GIAJ) were used in this numerical simulation. Moreover, within the most densely built-up districts in the metropolitan area of Osaka City, the urban grids of the innermost domain (shown in Section 2.2) were classified into three urban categories based on the most dominant type of building in each grid. In addition to the GIAJ LULC data, the Osaka City GIS polygon data, as shown above, were used for this classification. The urban grids were classified into three categories, as shown in Figures 1(c) and (d): commercial and business grids that mainly consisted of commercial and office buildings (hereafter C), residential grids that predominantly consisted of fireproof apartments (Rr), and residential grids that were chiefly covered by wooden detached dwellings (Rw). The urban grids in the area outside Osaka City, in the innermost domain, and those in the outer domains were classified as Rw in this study.

3. Results

3.1. Surface air temperature

Figure 3 shows the distribution of surface air temperatures observed at 1.5 m and simulated at 2 m above the ground surface (hereafter, surface air temperature) in August 2013, which was the hottest month during the study period. The CTRL roughly reproduced the horizontal distribution of air temperature (Figures 3(a) and (b)). The model also reproduced daytime temperature, but underestimated the temperature from midnight to morning in Osaka (Figure 3(c)). In this study, we defined the value of model results minus observation as bias (Table 2(a)). The root mean square error (RMSE) calculated using hourly data during 1 month was 1.6 °C (Table 2(b)). The histogram of simulated hourly temperature was similar to that of the observed temperature in Osaka (Figure 3(d)).

Figure 4 shows the temperature in February 2014, which was the coldest month during the study period. The CTRL roughly reproduced the horizontal distribution of air temperature (Figures 4(a) and (b)), but underestimated the temperature from midnight to morning in Osaka (Figure 4(c)). The RMSE was 1.5 °C (Table 2(b)). A histogram of the simulated hourly temperature produced a distribution with slightly lower temperatures compared to the observed temperatures in Osaka (Figure 4(d)).

The results of the bias and RMSE in all months are summarized in Tables 2(a) and (b), respectively. There was a unique feature regarding the biases of midnight–morning temperatures during the heating season, which tended to be smaller than in the cooling and interim seasons (Table 2(a)). The reason for this is discussed in Section 4. The RMSEs tended to be large in daytime during the cooling and interim seasons, and in the morning during the heating season (Table 2(b)).

3.2. Electricity demand

Figure 5 shows the electricity demand in August 2013. The CTRL tended to overestimate the observed electricity demand in the entire region (Figures 5(a) and (b)). Figures 5(c)–(e) shows the diurnal variations of the observed and simulated electricity demand in the Rw, Rr, and C areas, respectively. In these figures, grey shades indicate the range between the minimum and maximum electricity demands recorded in each urban category. The grey dashed line shows the electricity demand at the

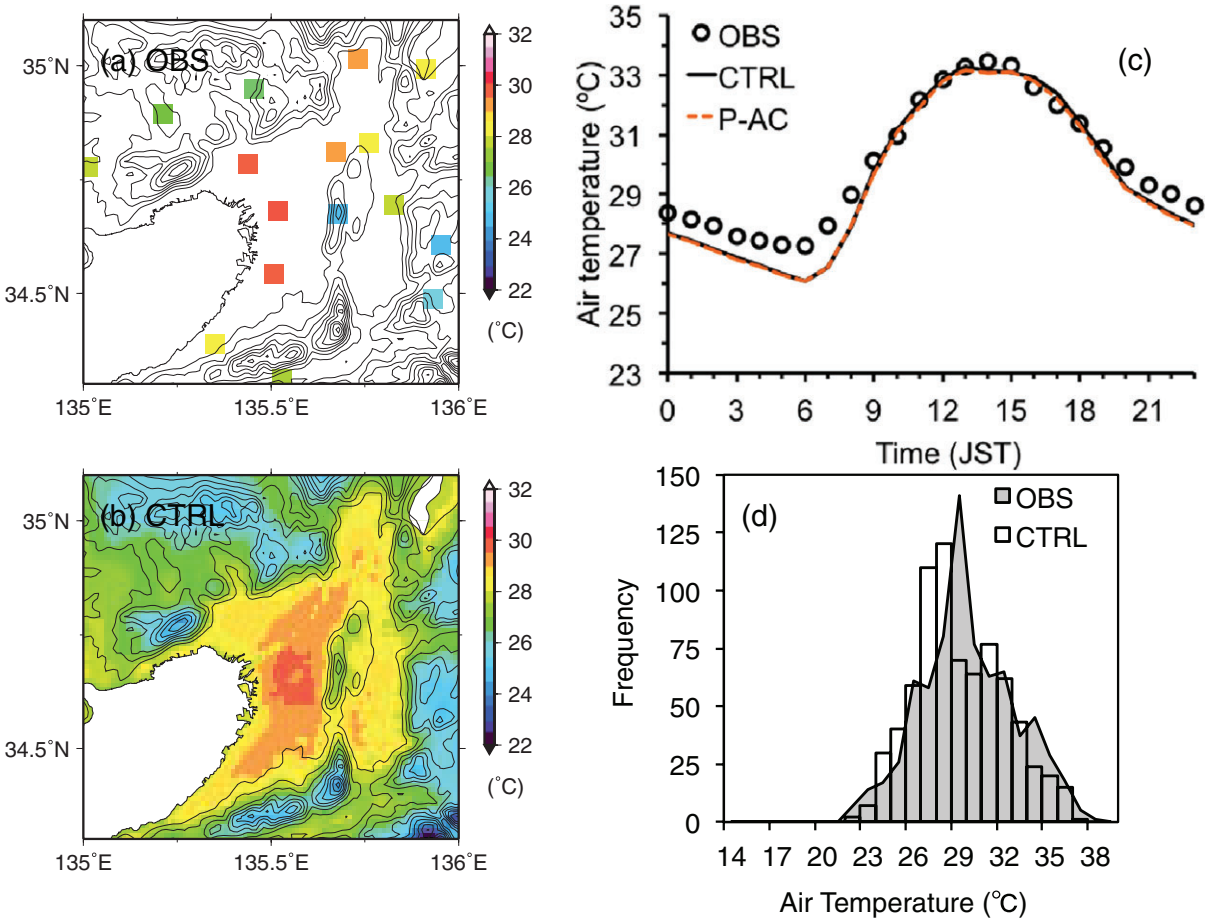

Figure 3. Horizontal distribution of surface air temperatures (a) observed at the AMeDAS site and (b) simulated by the WRF-BEP+BEM model [the control simulation (CTRL) is shown in Section 2.2], averaged for August 2013. (c) Diurnal variation and (d) frequency of surface air temperatures, as observed at the Osaka AMeDAS site (circles and grey shading) and simulated by CTRL (solid line and white bars) and the partial AC simulation (P-AC, orange dashed line) during 0000–2300 JST (UTC+9h), averaged for August 2013.

reference observation point (Figure 1(d)), which was used to calculate bias and RMSE for electricity demand. The averaged result of the CTRL is shown as a black solid line in these figures. The CTRL tended to overestimate daytime electricity demand in all urban categories, i.e. Rw, Rr, and C (Figures 5(c)–(e)). The biases in Rw, Rr and C are shown in Table S1, Supporting information. In addition, the daily averaged RMSE for Rw, Rr, and C were +2.9 W floor m^{-2}, +6.4 W floor m^{-2}, and +6.8 W floor m^{-2}, respectively.

The overestimation by the CTRL is also apparent in the results for February 2014. Figures 6(a) and (b) shows the horizontal distribution of the electricity demand, and indicates that the CTRL overestimated the actual demand. The model overestimated from early evening to late morning, all day, and during the daytime in Rw, Rr, and C, respectively (Table S1(c)–(d)). The biases in Rw, Rr and C are shown in Table S1. The averaged RMSE for Rw, Rr, and C were +4.6 W floor m^{-2}, +11.2 W floor m^{-2}, and +6.2 W floor m^{-2}, respectively.

The diurnal variation in the RMSE values in Rw, Rr, and C in each month are shown in Figure 7. In residential areas (i.e. Rw and Rr), notable errors were apparent in daytime during the cooling season and midnight–morning during the heating season (Figures 7(a) and (b)), which are periods with an increased AC load. In contrast, in C-classified areas, notable errors were apparent in daytime (Figure 7(c)), which corresponded to the time when AC systems were in operation (Table 1).

Here, we describe the monthly total electricity demand in the 12 districts around Osaka City ($\sum E_c$) as follows:

$$\sum E_c = \sum_{j=1}^{l} \sum_{i=1}^{k} E_c(i,j) \quad (3)$$

Here, i and j indicate hours and station numbers, respectively; k and l indicate the total hours in each month (24 × day number of the month) and total number of stations (12), respectively. Table 3 shows the ratio of simulated $\sum E_c^{CTRL}$ (kWh) over the 12 observation points in the Osaka City area to the observed $\sum E_c^{OBS}$ (hereafter CTRL/OBS). The values of the CTRL/OBS were over 1.0 in all months, indicating that the CTRL clearly overestimated the observed values. In particular, remarkable overestimations of more than 2.0 were apparent in the heating season, which were larger than the overestimations in the cooling season.

Table 2. (a) Air temperature difference (bias) between the CTRL and observations at the Osaka AMeDAS site. The blue and red numbers indicate biases of less than −1.5 °C and more than +1.5 °C, respectively. (b) Root mean square error (RMSE) at the Osaka AMeDAS site. The red numbers indicate a difference of more than +2.0 °C.

(a)

JST (UTC+9h)	0	1	2	3	4	5	6	7	8	9	10	11	12	13	14	15	16	17	18	19	20	21	22	23	Average
April	−0.9	−0.7	−0.7	−0.8	−0.8	−0.8	−1.0	−1.2	−0.9	−0.6	−0.5	−0.3	−0.2	−0.3	−0.1	0.5	0.5	0.4	0.2	−0.2	−0.6	−0.7	−1.0	−0.9	**−0.5**
May	−0.3	−0.3	−0.2	−0.3	−0.6	−0.6	−1.0	−0.9	−0.3	0.0	0.0	0.2	0.1	0.1	−0.1	−0.1	0.4	0.2	−0.1	−0.5	−0.6	−0.7	−0.5	−0.4	**−0.3**
June	0.3	0.2	0.1	−0.1	−0.1	−0.1	−0.3	−0.2	0.2	0.6	0.7	0.7	0.9	0.7	0.4	0.2	0.1	0.4	0.3	0.3	0.4	0.2	0.2	0.2	**0.3**
July	−1.1	−1.1	−1.1	−1.0	−1.1	−1.1	−1.2	−1.0	−0.6	−0.1	0.3	0.5	0.3	0.5	0.2	0.0	0.2	0.8	0.7	0.2	−0.6	−0.7	−1.0	−1.1	**−0.4**
August	−0.8	−0.7	−0.8	−0.7	−0.8	−1.0	−1.2	−1.4	−1.1	−0.3	0.2	−0.1	0.0	0.0	−0.3	−0.2	0.3	0.4	0.0	−0.2	−0.7	−0.5	−0.7	−0.6	**−0.5**
September	0.7	0.7	0.7	0.6	0.5	0.4	0.2	−0.1	0.2	1.0	1.3	1.4	**1.8**	**1.7**	**1.5**	1.4	1.3	1.2	0.9	0.8	0.6	0.6	0.7	0.7	**0.9**
October	0.0	0.0	0.0	0.0	−0.1	−0.2	−0.4	−0.8	−0.8	−0.2	0.3	0.7	1.0	1.1	1.0	0.9	0.7	0.4	0.3	0.2	0.1	0.0	0.1	0.0	**0.2**
November	−0.9	−1.0	−1.1	−1.3	−1.3	**−1.6**	**−1.7**	**−1.9**	**−2.3**	**−1.8**	−0.7	−0.4	−0.2	−0.2	0.2	0.3	0.2	0.0	−0.5	−0.5	−0.5	−0.5	−0.7	−0.7	**−0.8**
December	−1.1	−1.2	**−1.5**	**−1.9**	**−1.9**	**−1.9**	**−2.1**	**−2.3**	**−2.5**	**−2.7**	**−1.8**	−1.2	−0.8	−0.4	−0.2	−0.1	−0.1	−0.4	−0.8	−1.0	−0.8	−0.9	−0.9	−0.9	**−1.2**
January	−0.8	−0.8	−1.0	−1.2	−1.2	−1.4	**−1.5**	**−1.8**	**−2.3**	**−2.4**	**−1.6**	−1.0	−0.4	0.0	−0.1	0.1	0.1	−0.1	−0.6	−1.0	−0.6	−0.6	−0.6	−0.7	**−0.9**
February	−0.6	−0.9	−0.8	−1.2	−1.2	−1.3	−1.4	**−1.8**	**−2.3**	**−1.7**	−0.9	−0.3	0.3	0.2	0.2	0.1	0.1	0.1	−0.2	−0.4	−0.2	−0.3	−0.4	−0.3	**−0.6**
March	−0.8	−0.8	−0.9	−1.0	−1.0	−0.9	−0.8	−1.1	−0.9	−0.4	−0.1	0.2	0.1	0.3	0.6	0.4	0.1	0.2	0.1	−0.3	−0.3	−0.5	−0.7	−0.8	**−0.4**

(b)

JST (UTC+9h)	0	1	2	3	4	5	6	7	8	9	10	11	12	13	14	15	16	17	18	19	20	21	22	23	**Ave**rage
April	1.5	1.4	1.5	1.6	1.6	1.6	1.6	1.7	1.6	1.8	1.6	1.9	**2.1**	1.9	**2.2**	**2.3**	**2.3**	**2.0**	1.7	1.9	1.9	1.7	1.6	1.6	**1.8**
May	1.5	1.4	1.4	1.5	1.6	1.4	1.6	1.6	1.1	1.0	1.5	1.8	1.5	1.3	1.5	1.8	1.8	1.6	1.4	1.7	1.8	1.6	1.6	1.6	**1.5**
June	1.7	1.6	1.4	1.3	1.3	1.3	1.5	1.5	1.4	1.5	1.7	1.9	**2.4**	**2.5**	**2.8**	**2.6**	**2.8**	**2.3**	**2.3**	**2.1**	**2.2**	**2.0**	1.9	1.8	**1.9**
July	1.8	1.7	1.7	1.7	1.6	1.6	1.7	1.6	1.5	1.6	**2.1**	**2.0**	1.9	**2.0**	1.8	1.9	1.7	**2.2**	**2.4**	**2.0**	**2.0**	1.9	1.9	1.9	**1.8**
August	1.4	1.4	1.4	1.5	1.5	1.5	1.7	1.7	1.4	1.1	1.6	1.8	1.9	**2.0**	**2.1**	**2.2**	**2.1**	**2.0**	1.8	1.6	1.5	1.5	1.4	1.4	**1.6**
September	**2.0**	1.9	1.7	1.6	1.6	1.5	1.6	1.9	**2.0**	**2.3**	**2.5**	**2.7**	**3.0**	**3.4**	**3.3**	**3.3**	**3.2**	**3.1**	**2.8**	**2.7**	**2.4**	**2.2**	**2.1**	**2.0**	**2.4**
October	1.4	1.5	1.5	1.4	1.5	1.5	1.6	1.7	1.8	**2.0**	**2.1**	**2.4**	**2.6**	**2.7**	**2.6**	**2.4**	**2.1**	**2.0**	1.8	1.6	1.5	1.4	1.4	1.3	**1.8**
November	1.6	1.6	1.7	1.6	1.6	**2.0**	**2.2**	**2.4**	**2.8**	**2.7**	**2.3**	1.9	1.9	1.8	1.8	1.7	1.4	1.5	1.5	1.3	1.2	1.3	1.3	1.3	**1.8**
December	1.7	1.8	**2.1**	**2.5**	**2.4**	**2.4**	**2.6**	**2.7**	**3.0**	**3.4**	**2.8**	**2.0**	1.6	1.5	1.2	1.0	1.2	1.1	1.5	1.6	1.4	1.4	1.4	1.5	**1.9**
January	1.8	1.8	1.9	1.9	1.8	**2.0**	**2.1**	**2.4**	**2.9**	**3.2**	**2.2**	1.9	**2.0**	**2.1**	**2.0**	**2.1**	**2.0**	1.9	**2.0**	**2.0**	1.7	1.6	1.7	1.8	**2.0**
February	1.6	1.7	1.7	1.9	1.9	**2.0**	**2.1**	**2.3**	**2.7**	**2.2**	1.5	1.3	1.4	1.4	1.5	1.2	1.1	1.0	0.8	0.9	0.9	1.0	1.3	1.3	**1.5**
March	1.6	1.6	1.7	1.9	1.8	**2.1**	**2.1**	**2.5**	**2.5**	**2.0**	1.8	1.9	**2.2**	**2.1**	**2.1**	**2.1**	**2.1**	1.8	1.6	1.5	1.4	1.5	1.6	1.6	**1.9**

Int. J. Climatol. **37** (Suppl.1): 1035–1052 (2017)

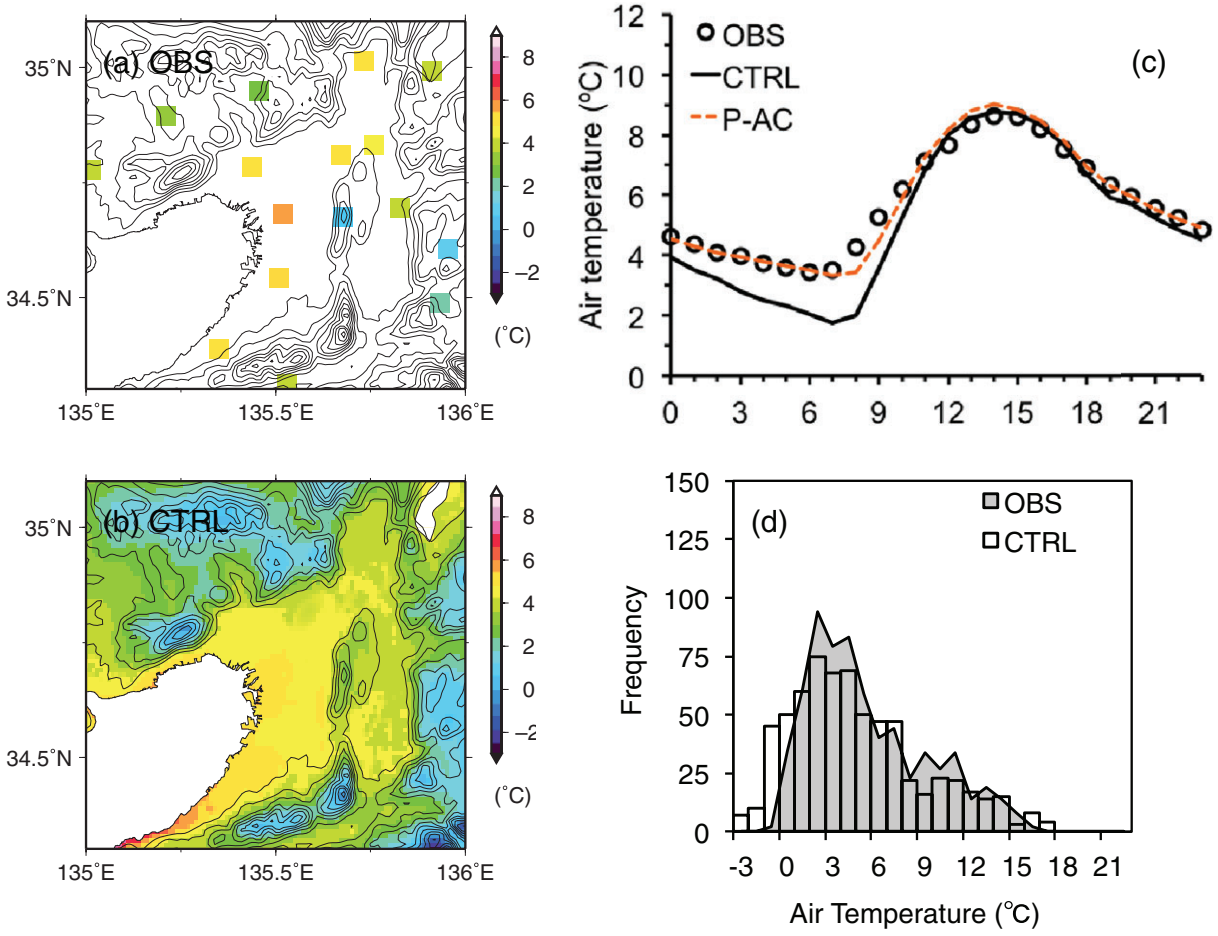

Figure 4. Horizontal distribution of surface air temperatures (a) observed at the AMeDAS site and (b) simulated by the WRF-BEP+BEM model (the CTRL case is shown in Section 2.2), averaged for February 2014. (c) Diurnal variation and (d) frequency of surface air temperatures observed at the Osaka AMeDAS site (circles and grey shading) and simulated by CTRL (solid line and white bars) and the partial AC simulation (P-AC, orange dashed line) during 0000–2300 JST (UTC+9h), averaged for February 2014.

4. Discussion

4.1. Investigation of the overestimation of electricity demand by the CTRL

Previous results suggested that the overestimations of electricity demand by the CTRL were caused by the use of AC systems. The CTRL assumed a central AC system, rather than partial AC, and therefore the CTRL could not distinguish between rooms with and without individual AC units, as explained in Section 2.2. Accordingly, AC is operating in all the buildings, floors, and rooms in the CTRL. This is not a common feature in Japan, where individual AC units are mainly used (e.g. Ihara *et al.,* 2008; Kikegawa *et al.,* 2014). Thus, this central AC setting would have contributed to the overestimations. To prevent this overestimation of AC use and improve the reproducibility of the electricity demand, we introduced the following three parameters, considering the use of partial AC systems: (1) the ratio of abandoned houses/buildings to all the houses/buildings in a city block (parameter *a*); (2) the ratio of air-conditioned floor area to total floor area (parameter *b*); and (3) the ratio of AC usage for cooling or heating to all the cooling and heating equipment (e.g. heaters, fireplaces, and other equipment) (parameter *c*). With regard to parameter *a*, there are many abandoned houses in Japan, which represents a social problem for the country. According to Osaka City (2015), the proportion of abandoned houses among the city's housing stock is 0.172, and it is reasonable to assume that they do not use AC. For parameter *b*, the ratio of air-conditioned floor area to total floor area was reported by Kikegawa *et al.* (2014), with values of 0.71 and 0.05 in office and residential areas, respectively. Salamanca *et al.* (2013) also considered such a ratio, and showed that the BEP+BEM was able to reproduce the diurnal profile of AC electricity demand when the value was set to 0.65 for the city of Phoenix in the United States. With regard to parameter *c*, most people use AC as cooling equipment in the cooling season. However, not many people use AC as heating equipment in the heating season, because there are many other types of heating equipment available, such as heaters.

4.2. Improvement of the BEP+BEM model for a Japanese megacity

To examine the effectiveness of the three parameters on electricity demand, we ran a sensitivity check experiment,

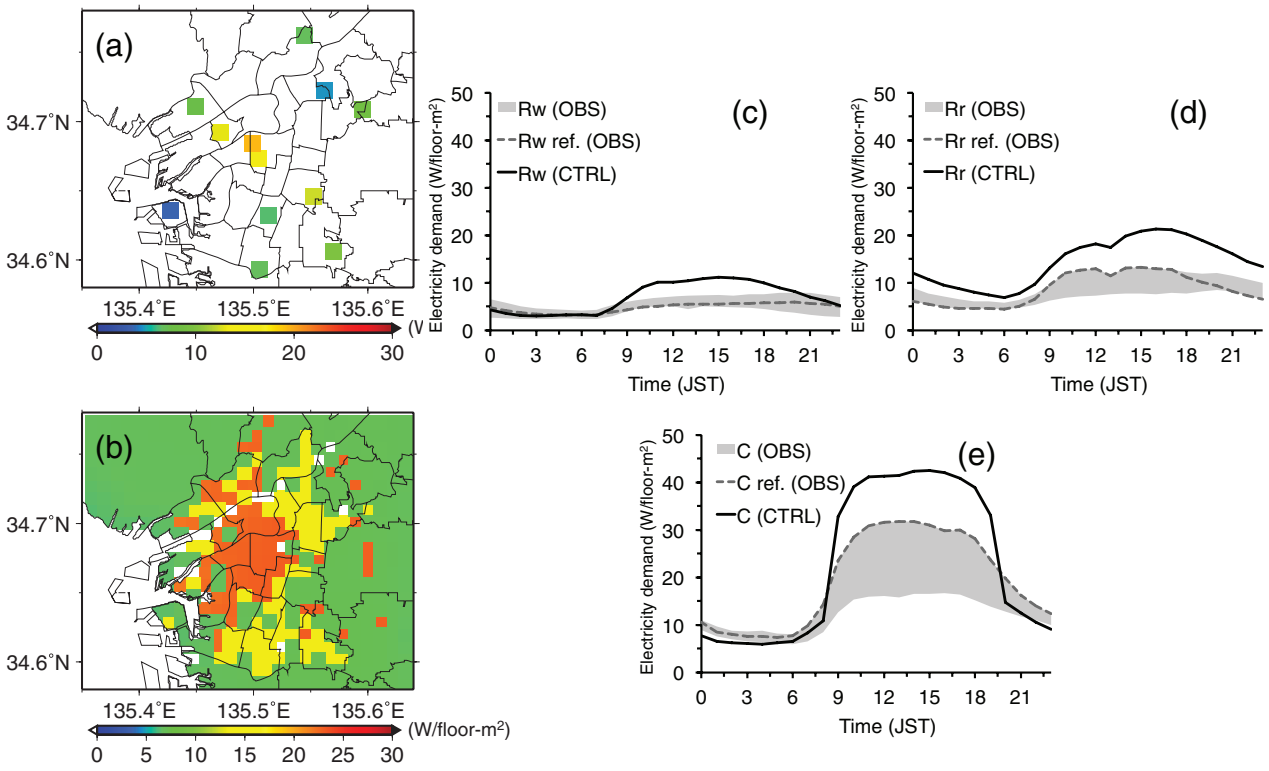

Figure 5. Horizontal distribution of the electricity demand (a) recorded at 12 sites and (b) simulated by the WRF-BEP+BEM model (the CTRL case is shown in Section 2.2) averaged for August 2013. Diurnal variations in electricity demand observed in (c) Rw, (d) Rr, and (e) C areas (grey dashed lines and grey shades) and simulated by the CTRL (black solid lines) during 0000–2300 JST (UTC+9h), averaged for August 2013.

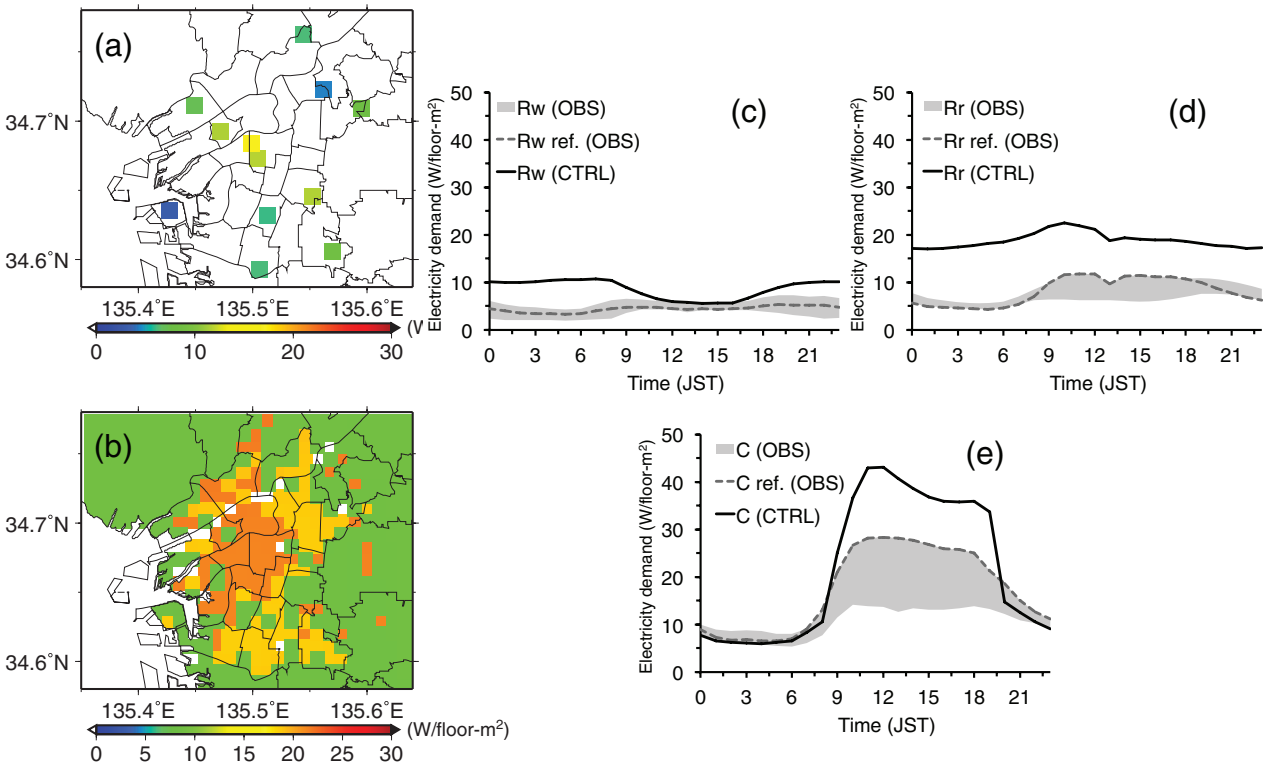

Figure 6. Horizontal distribution of the electricity demand (a) observed at 12 sites and (b) simulated by the WRFBEP+BEM model (the CTRL case is shown in Section 2.2), averaged for February 2014. Diurnal variations in electricity demand observed at (c) Rw, (d) Rr, and (e) C areas (grey dashed lines and grey shading), and simulated by the CTRL (black solid lines) during 0000–2300 JST (UTC+9h) averaged for February 2014.

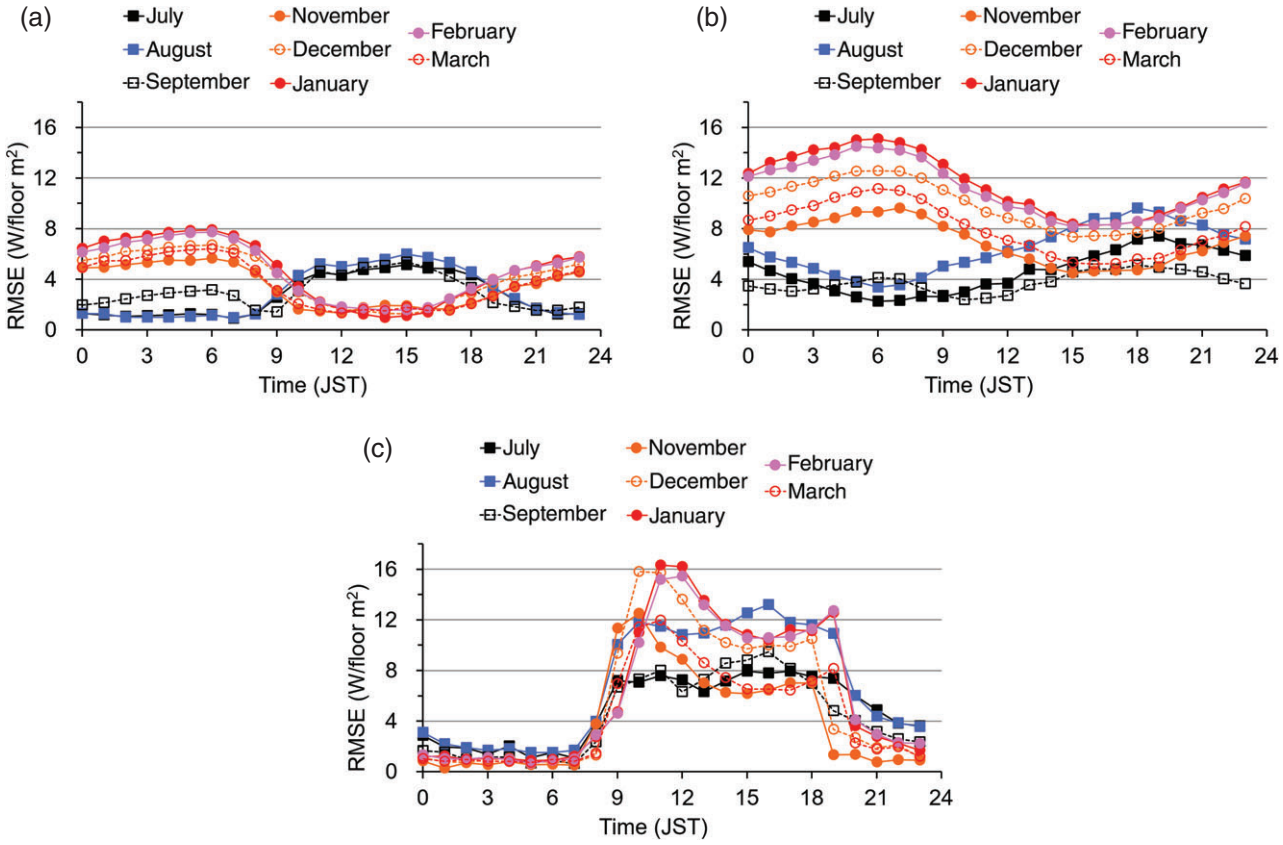

Figure 7. Diurnal variations in root mean square error (RMSE) of electricity demand between the CTRL and observations during cooling (cold colours) and heating seasons (warm colours) at (a) Rw, (b) Rr, and (c) C reference sites.

Table 3. Ratio of simulated total electricity demand $\sum E_C^{CTRL}$ (CTRL) and $\sum E_C^{P\text{-}AC}$ (P-AC) over the 12 observation sites in Osaka (Figure 1) to observed $\sum E_C^{OBS}$ (simulations/observation).

	April	May	June	July	August	September	October	November	December	January	February	March
CTRL/OBS	No use of AC system			1.45	1.55	1.46	–	1.78	1.97	2.05	2.02	1.80
P-AC/OBS	No use of AC system			1.16	1.20	1.19	–	1.25	1.22	1.21	1.21	1.21

hereafter referred to as the partial AC simulation (P-AC). Specifically, the equation describing modified electricity demand ($E_C^{P\text{-}AC}$) was as follows:

$$E_C^{P\text{-}AC} = \frac{1}{COP}\left(H_{out}^{P\text{-}AC} + E_{out}^{P\text{-}AC}\right) \quad (4a)$$

We inserted the three parameters discussed above into the modified sensible heat ($H_{out}^{P\text{-}AC}$) and latent heat ($E_{out}^{P\text{-}AC}$) supplied from the system as follows:

$$H_{out}^{P\text{-}AC} = H_{out} * (1-a) * b * c, \quad (4b)$$

$$E_{out}^{P\text{-}AC} = E_{out} * (1-a) * b * c \quad (4c)$$

Here, $a = 0.172$ (Osaka City, 2015), $b = 0.71$ (Kikegawa *et al.*, 2014), and $c = 1.0$ (for the cooling season) or 0.6 (for the heating season) (Internet survey of 500 men and women aged 20 years and older, January 2012). Other model descriptions were unchanged.

The electricity demand simulated by the P-AC in August 2013 is shown in Figure 8, which demonstrates that the P-AC results agreed well with the observations in all urban categories compared to the CTRL shown in Figure 5. The biases in Rw, Rr, and C are shown in Table S2. In addition, the averaged RMSE for Rw, Rr, and C were +3.3 W floor m^{-2}, +1.4 W floor m^{-2}, and 3.7 W floor m^{-2}, respectively. These biases and RMSE values were much lower than those of the CTRL (Figure 7 and Table S1).

This improvement was also apparent in the results for February 2014, shown in Figure 9. The biases in Rw, Rr, and C are shown in Table S2. The averaged RMSE for Rw, Rr, and C were 1.6 W floor m^{-2}, 0.9 W floor m^{-2}, and 1.6 W floor m^{-2}, respectively. As with the August 2013 results, these biases and RMSE values were also lower than those of the CTRL (Figure 6). Figure 10 shows that, compared

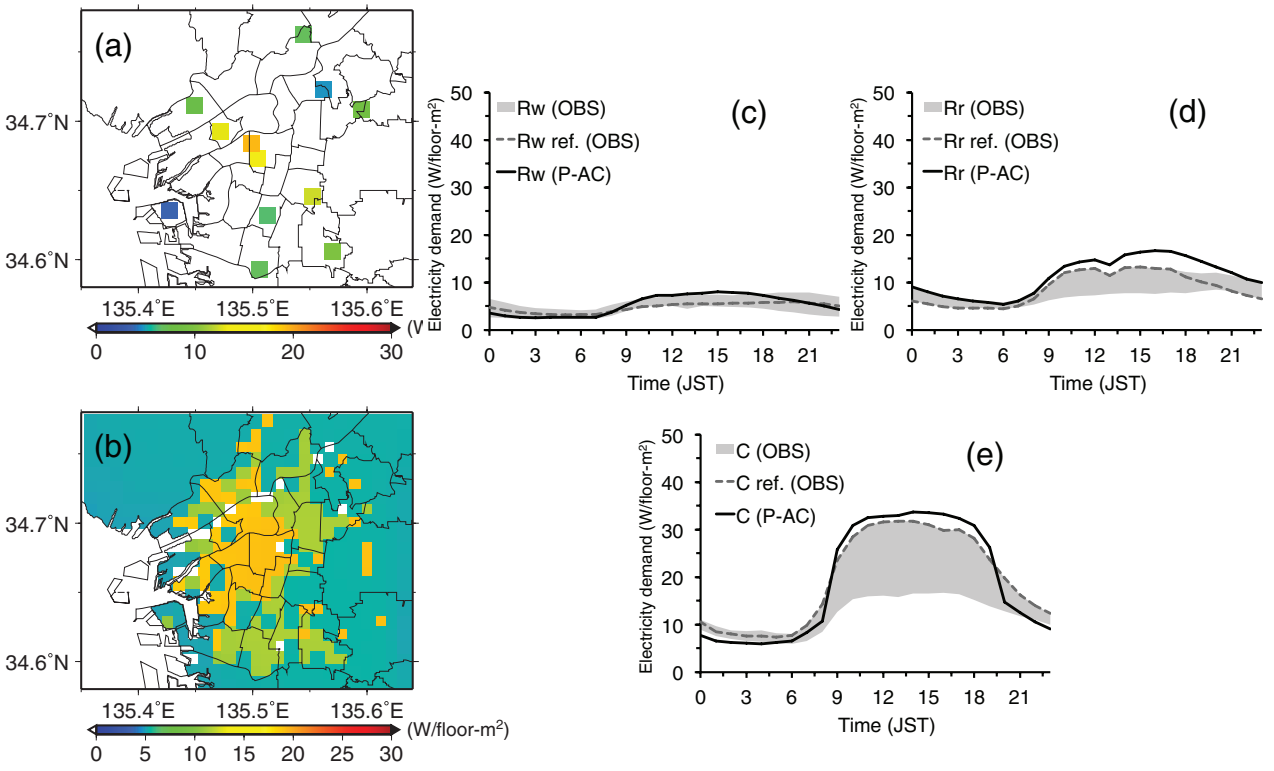

Figure 8. Same as Figure 5, but for the results of the partial air-conditioning (P-AC) case.

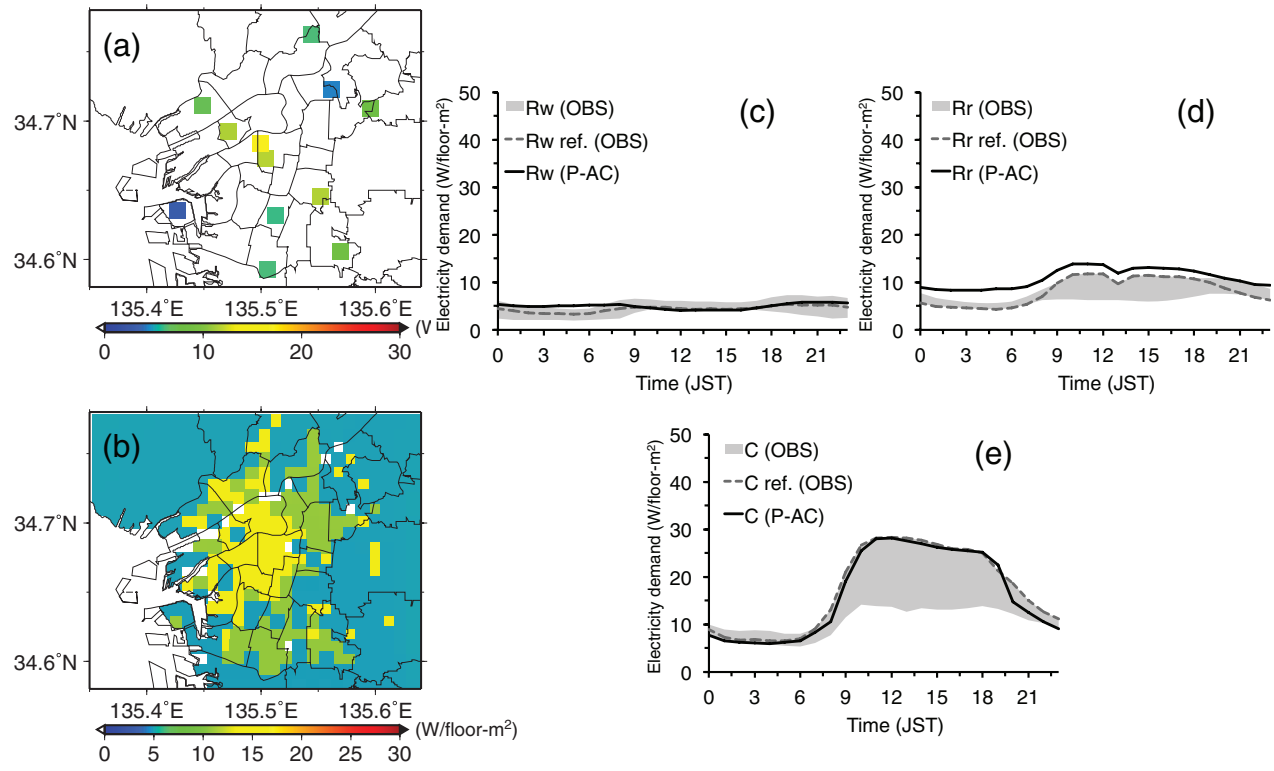

Figure 9. Same as Figure 6, but for the results of the P-AC case.

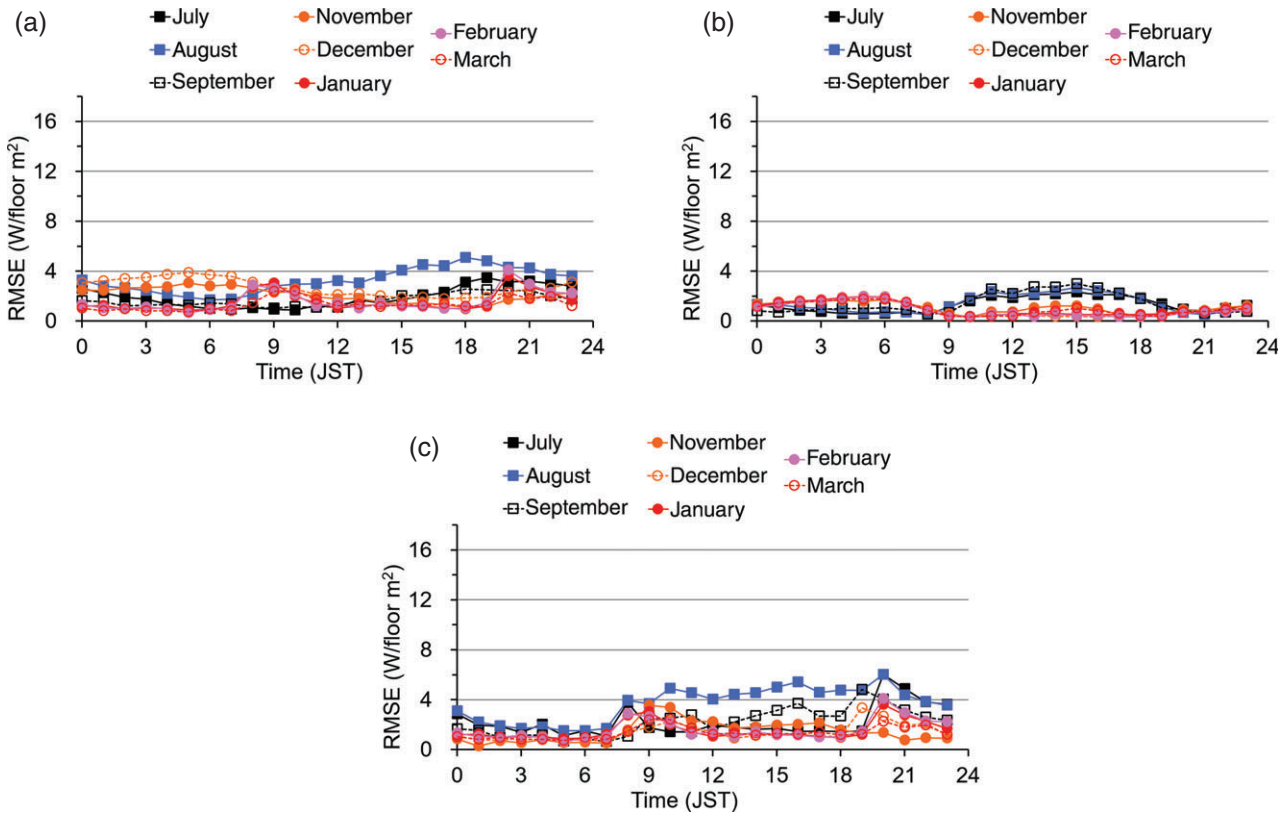

Figure 10. Same as Figure 7, but for the results of the P-AC case.

to the CTRL, the P-AC reproduced the electricity demand in Rw, Rr, and C reasonably well, not only in August and February but also for the other months.

The underestimation of surface air temperature by the CTRL during midnight-morning in the heating season, as described in Section 3, was also reduced by the P-AC (Tables 2 and 4). In general, sensible heat is pumped by a heat-pumped AC system from the outside of a building to the interior in the heating season, which results in negative sensible heat emissions outside. As the AC is operated in all buildings, floors, and rooms in the CTRL, it is very likely that the sensible heat pumped from the outside to inside (negative sensible heat release) is overestimated, which contributes to underestimation of air temperature simulated by the CTRL. Ohashi *et al.* (2016b) observed that surface air temperature on weekdays in Osaka was significantly lower than that on weekends (including holidays) during the winter heating season. They suggested that this temperature difference was caused by differences in human activity, i.e. the use of heat-pumped AC systems. That is, the active use of a heat-pumped AC caused negative sensible heat, which contributed to lower temperatures on weekdays. The observations reported by Ohashi *et al.* (2016b) support the conclusions of this study.

As in the heating season, electricity demand in the cooling season was also overestimated by the CTRL. However, this overestimation contributed little to the surface air temperature, unlike in the heating season. It is possible that the difference in the effects of overestimation on surface air temperature between the heating and cooling seasons were due to the following reasons. (1) The overestimation of the electricity demand (anthropogenic heat due to use of AC) mainly occurred during daytime in the cooling season, and at night in the heating season (Figure 7). Thus, these overestimations in the cooling and heating seasons mainly contributed to the temperatures during daytime and nighttime, respectively. In general, the effects of anthropogenic heat on surface air temperature were much clearer at night than in the daytime due to difference in mixed layer heights, with the same amount of anthropogenic heat released in both periods. (2) As described in Section 4.2, most people use AC as cooling equipment in the cooling season, but not all people use AC as heating equipment in the heating season, because there are many heating equipment options available. In the P-AC case, we set the parameter c to 1.0 in the cooling season and 0.6 in the heating season. However, this parameter was assumed to be 1.0 in both seasons in the CTRL case. Thus, the difference in anthropogenic heating due to the use of AC between observations and simulations in the heating season was larger than in the cooling season, which contributed to the difference in the effects of electricity demand on temperature. The positive bias in the heating season was higher than in the cooling season (Figure 7), which supports the explanation given above.

4.3. Total electricity demand in Osaka City

Here, we discuss the monthly total electricity demand in the 12 districts around Osaka City. As described in Section 3, the CTRL clearly overestimated the observed

Table 4. Same as Table 2, but for the results of the partial air-conditioning (P-AC) case.

(a)

JST (UTC+9h)	0	1	2	3	4	5	6	7	8	9	10	11	12	13	14	15	16	17	18	19	20	21	22	23	**Ave**rage
April	Same as Table 2(a)																								
May	Same as Table 2(a)																								
June	Same as Table 2(a)																								
July	−1.1	−1.1	−1.1	−1.0	−1.0	−1.0	−1.1	−0.8	−0.5	−0.2	0.1	0.3	0.3	0.4	0.1	−0.1	0.2	0.7	0.5	0.0	−0.6	−0.8	−1.0	−1.1	**−0.4**
August	−0.8	−0.8	−0.8	−0.8	−0.9	−1.0	−1.2	−1.4	−1.0	−0.5	0.1	−0.2	0.0	−0.1	−0.4	−0.2	0.2	0.2	−0.1	−0.4	−0.7	−0.6	−0.7	−0.7	**−0.5**
September	0.7	0.7	0.7	0.7	0.6	0.6	0.5	0.1	0.4	1.0	1.4	**1.5**	**1.7**	**1.8**	1.4	**1.5**	1.3	1.2	0.9	0.7	0.7	0.6	0.7	0.7	**0.9**
October	Same as Table 2(a)																								
November	−0.4	−0.4	−0.4	−0.4	−0.3	−0.3	−0.3	−0.5	−0.9	−0.7	−0.2	−0.2	−0.1	−0.1	0.3	0.3	0.2	0.2	−0.3	−0.4	−0.3	−0.3	−0.5	−0.4	**−0.3**
December	−0.5	−0.5	−0.5	−0.5	−0.4	−0.3	−0.4	−0.5	−0.7	−1.1	−0.7	−0.7	−0.5	−0.3	0.0	0.1	0.1	0.0	−0.3	−0.5	−0.5	−0.6	−0.5	−0.5	**−0.4**
January	0.3	0.4	0.4	0.4	0.4	0.1	0.1	0.0	−0.5	−0.7	−0.5	−0.3	0.1	0.3	0.2	0.1	0.3	0.2	−0.1	−0.2	−0.1	−0.2	−0.1	0.0	**0.0**
February	0.0	−0.1	0.0	−0.1	0.1	0.1	0.1	−0.2	−0.8	−0.8	−0.3	0.1	0.5	0.4	0.4	0.2	0.3	0.3	0.0	0.0	0.0	−0.1	0.0	0.1	**0.0**
March	−0.5	−0.4	−0.3	−0.3	−0.2	0.0	0.1	−0.1	−0.3	0.0	0.2	0.3	0.3	0.4	0.6	0.5	0.2	0.2	0.2	−0.1	−0.2	−0.3	−0.6	−0.5	**0.0**

(b)

JST (UTC+9h)	0	1	2	3	4	5	6	7	8	9	10	11	12	13	14	15	16	17	18	19	20	21	22	23	Average
April	Same as Table 2(b)																								
May	Same as Table 2(b)																								
June	Same as Table 2(b)																								
July	1.8	1.7	1.7	1.7	1.6	1.5	1.6	1.5	1.5	1.5	1.9	1.9	1.7	1.9	1.9	**2.0**	1.6	**2.2**	**2.3**	**2.0**	**2.0**	1.9	1.9	1.9	**1.8**
August	1.4	1.4	1.4	1.6	1.6	1.5	1.7	1.8	1.4	1.1	1.6	1.7	1.9	**2.0**	**2.1**	**2.2**	**2.1**	**2.0**	1.8	1.6	1.5	1.5	1.4	1.4	**1.7**
September	1.9	1.8	1.6	1.5	1.5	1.5	1.5	1.6	1.9	**2.3**	**2.5**	**2.7**	**2.8**	**3.5**	**3.2**	**3.3**	**3.3**	**3.0**	**2.9**	**2.7**	**2.5**	**2.1**	**2.0**	1.9	**2.3**
October	Same as Table 2(b)																								
November	1.3	1.2	1.2	1.1	0.9	1.0	1.1	1.1	1.5	1.8	1.9	1.8	1.9	1.7	1.7	1.7	1.4	1.5	1.4	1.2	1.2	1.2	1.1	1.2	**1.4**
December	1.3	1.3	1.3	1.3	1.2	1.3	1.5	1.5	1.8	1.8	1.9	1.6	1.4	1.4	1.2	1.0	1.3	1.1	1.3	1.4	1.3	1.3	1.2	1.3	**1.4**
January	1.5	1.4	1.4	1.3	1.2	1.3	1.5	1.5	1.5	1.6	1.7	1.9	**2.1**	**2.2**	**2.0**	**2.2**	1.9	**2.0**	1.9	1.8	1.6	1.5	1.6	1.5	**1.7**
February	1.3	1.2	1.2	1.1	1.2	1.2	1.2	1.2	1.4	1.4	1.2	1.3	1.5	1.5	1.5	1.2	1.1	1.1	0.8	0.9	0.9	1.0	1.2	1.3	**1.2**
March	1.4	1.3	1.3	1.5	1.5	1.7	1.9	**2.0**	**2.2**	1.9	1.9	1.9	**2.2**	**2.2**	**2.1**	**2.2**	**2.1**	1.8	1.6	1.4	1.4	1.4	1.5	1.4	**1.7**

Int. J. Climatol. **37** (Suppl. 1): 1035–1052 (2017)

monthly total electricity demand. These overall overestimations were reduced in the P-AC case, but some overestimation remained.

As described in Section 4.2, the biases at the reference C site in August 2013 and February 2014 by the P-AC case were −0.3 and −0.9 W floor m^{-2}, respectively, which indicates that the P-AC provided results that agreed well with observations at the reference points. At the reference C site, the proportion of the area covered by C category buildings to the total area (hereafter occupant ratio) was about 90%, which was close to the simulation setting of 100%. Therefore, the P-AC reproduced the observations well at this site (specifically P-AC /OBS = 0.98). In the same way, the P-AC case could also reproduce the observations at other C sites (Figure 1(d)), with occupant ratios of about 70% (P-AC /OBS = 1.09). In contrast, the occupant ratio at the reference Rr site was about 60% (the remaining 40% was Rw), which was quite different from the simulation setting (100%). This difference would contribute to the overestimation of P-AC/OBS = 1.30. To summarize, the P-AC case tended to overestimate electricity demand at stations where the actual occupant ratio was notably different from the simulation ratio of 100%. These overestimations due to the difference of the occupant ratio at each site were accumulated, and contributed to the overestimation of monthly total electricity demand in Osaka City. To solve this, it is necessary to take into account the urban sub-grid parameterization for the heterogeneous urban category in all urban grids. For example, it would be better to set both occupant ratios of Rr (60%) and Rw (40%) for simulations in the case of the reference Rr site, and calculate electricity demands separately in both urban categories in the same grid. This model modification is an issue for future studies.

In addition, we used 0.71 as the ratio of air-conditioned floor area to total floor area (parameter *b*) in not only C but also the Rr and Rw categories, as described in Section 4.2. However, Kikegawa *et al.* (2014) set the ratio as 0.71 and 0.05 in business and residential areas, respectively. This difference in the parameter, between 0.71 in this study and 0.05 in the previous study for a residential area, is likely to be the reason for the overestimation in Rr and Rw by the P-AC. However, it should be noted that the overestimation in the Rw sites made little contribution to the monthly total value, because the electricity demand in Rw sites was smaller than that in C and Rr sites (Figures 5 and 6).

4.4. Future work

As discussed above, the consideration of an urban sub-grid parameterization for the heterogeneous urban category in all urban grids is effective in reproducing the horizontal distribution and total electricity demand in the entire area. The numerical simulation with higher horizontal resolution is also effective because this simulation can better resolve the heterogeneous urban category in urban grid. These will be the focus of a study in the near future. In addition, as described in Section 2.2, the BEP+BEM does not consider anthropogenic heat due to traffic, and cannot calculate the temporal variation in the COP. Moreover, the model cannot deal with the situation during holidays. In addition, not only electric AC, but gas AC should also be considered in office areas in future studies. The consideration of gas AC influences the parameter *c*: the ratio of AC usage for cooling or heating to all of the cooling and heating equipment. An improvement of these features would increase the reproducibility of electricity demand and urban air temperature, as is the case with the WRF-CM-BEM developed by Kikegawa *et al.* (2014). It is important to improve the model to ensure that it is as simple as possible to use for climate simulations to save computation costs and avoid the confusing settings associated with having many parameters.

5. Conclusion

The basic performance of a RCM coupled with an UCM and BEM had not been sufficiently validated by previous studies. In this study, we validated urban air temperature and electricity demand by a year-round numerical simulation using an RCM coupled with a UCM and BEM (WRF-BEP+BEM) in the Asian megacity of Osaka, Japan. In this validation, we investigated not only diurnal variation, but also the horizontal distribution and total energy demand in the urban area.

The control (CTRL) simulation, which was based on the use of central AC systems, tended to underestimate the surface air temperatures observed at Osaka City from midnight to morning during all seasons. In particular, the CTRL remarkably underestimated surface air temperatures during the winter heating season by over 2 °C. In addition, the CTRL substantially overestimated the electricity demand in Osaka City during periods when the AC load increased in both the cooling and heating seasons.

This underestimation of midnight-morning temperature in the heating season, and the overestimation of electricity demand in both seasons, was caused by the overestimation of AC use in the model, because central AC systems are not common in business and residential areas in Japan. To prevent this overestimation and improve the reproducibility of the temperatures and electricity demands, we took the following three parameters into account: (1) the ratio of abandoned houses/buildings to all houses/buildings in a city block, (2) the ratio of air-conditioned floor area to the total floor area, and (3) the ratio of AC usage for cooling or heating to the use of all the cooling and heating equipment. In this new experiment, referred to as the P-AC, the incorporation of these parameters substantially reduced the underestimation of temperature and the overestimation of electricity demand. This suggests that the modified WRF-BEP+BEM used in this study is an effective tool to reproduce the year-round urban air temperature and electricity demand in a typical urban grid (e.g. the reference C site). This model would also be useful to project the future urban climate and electricity demand.

However, the P-AC tended to overestimate the monthly total electricity demand in the whole of Osaka City (e.g.

the ratio of simulation to observation: P-AC /OBS = 1.2 in August 2013) as with the CTRL case (CTRL/OBS = 1.5), even if we used the modified model. Additional analysis suggested that the P-AC tended to overestimate the electricity demand at stations where the actual occupant ratio of each urban category was notably different from the simulation ratio of 100%. To solve this, it would be necessary to take into account urban sub-grid parameterization for the heterogeneous urban category in all urban grids in the future.

We clearly identified the current level of WRF-BEP+BEM basic performance and identified the problems associated with climatologically simulating urban air temperature and electricity demand by a year-round simulation. The results will help to project future urban climate and energy demand in Asian mega cities. They will also be applicable to high-latitude cities in Europe and North America in future situations where AC systems are widely used.

Acknowledgements

We thank Prof. F. Salamanca of Arizona State University for helpful comment associated with the WRF−BEP+BEM. The observation was supported by JSPS KAKENHI Grant−in Aid for Scientific Research (B) Number 24360218. The numerical simulations were supported by the Environmental Research and Technology Development Fund (S−14) of the Ministry of the Environment, Japan, and JSPS KAKENHI Grant-in-Aid for Young Scientists (A) number 26702006. The numerical simulations were performed under the 'Interdisciplinary Computational Science Program' in the Center for Computational Sciences, University of Tsukuba. The free software package Generic Mapping Tools (GMT) was used in drawing the figures.

Supporting information

The following supporting information is available as part of the online article:

Table S1. The difference (bias) in electricity demand between the control simulation (CTRL) and observations at the (a) wooden detached dwellings (Rw), (b) fireproof apartments (Rr), and (c) commercial and office building (C) reference sites. The blue, red and pink numbers indicate less than −5.0, more than +5.0, and +10 W floor m^{-2}, respectively.

Table S2. Same as Table S1, but for the results of the P−AC case.

References

Adachi SA, Kimura F, Kusaka H, Duda MG, Yamagata Y, Seya H, Nakamichi K, Aoyagi T. 2014. Moderation of summertime heat island phenomena via modification of the urban form in the Tokyo metropolitan area. *J. Appl. Meteorol. Climatol.* **53**: 1886−1900, doi: 10.1175/JAMC-D-13-0194.1.

Ashie Y, Vu Thanh C, Asaeda T. 1999. Building canopy model for the analysis of urban climate. *J. Wind Eng. Ind. Aerodyn.* **81**: 237−248, doi: 10.1016/S0167-6105(99)00020-3.

Best MJ, Grimmond CSB. 2015. Key conclusions of the first international urban land surface model comparison project. *Bull. Am. Meteorol. Soc.* **96**: 805−819, doi: 10.1175/BAMS-D-14-00122.1.

Bueno B, Norford L, Pigeon G, Britter R. 2011. Combining a detailed building energy model with a physically-based urban canopy model. *Bound.-Layer Meteorol.* **140**: 471−489, doi: 10.1007/s10546-011-9620-6.

Bueno B, Pigeon G, Norford LK, Zibouche K, Marchadier C. 2012. Development and evaluation of a building energy model integrated in the TEB scheme. *Geosci. Model Dev.* **5**: 433−448, doi: 10.5194/gmd-5-433-2012.

Chen F, Dudhia J. 2001. Coupling an advanced land−surface/hydrology model with the Penn State/NCARMM5 modeling system. Part I: Model description and implementation. *Mon. Weather Rev.* **129**: 569−585, doi: 10.1175/1520-0493(2001)129<0569:CAALSH>2.0.CO;2.

Crawley DB, Lawrie LK, Winkelmann FC, Buhl WF, Huang YJ, Pedersen CO, Strand RK, Liesen RJ, Fisher DE, Witte MJ, Glazer J. 2001. EnergyPlus: creating a new-generation building energy simulation program. *Energy Build.* **33**: 319−331, doi: 10.1016/S0378-7788(00)00114-6.

Dudhia J. 1989. Numerical study of convection observed during the winter monsoon experiment using a mesoscale two-dimensional model. *J. Atmos. Sci.* **46**: 3077−3107, doi: 10.1175/1520-0469(1989)046<3077:NSOCOD>2.0.CO;2.

Energy Conservation Center of Japan. 2005. Report of study on energy saving effects on urban heat island mitigation in 2004FY (title only in original language). Geo Hatchobori, Tokyo, Japan. (in Japanese).

Grimmond CSB, Blackett M, Best MJ, Barlow J, Baik J-J, Belcher SE, Bohnenstengel SI, Calmet I, Chen F, Dandou A, Fortuniak K, Gouvea ML, Hamdi R, Hendry M, Kawai T, Kawamoto Y, Kondo H, Krayenhoff ES, Lee S-H, Loridan T, Martilli A, Masson V, Miao S, Olsen K, Pigeon G, Porson A, Ryu Y-H, Salamanca F, Shashua-Bar L, Steeneveld G-J, Tombrou M, Voogt J, Young D, Zhang N. 2010. The international urban energy balance models comparison project: first results from phase 1. *J. Appl. Meteorol. Climatol.* **49**: 1268−1292, doi: 10.1175/2010JAMC2354.1.

Grimmond CSB, Blackett M, Best MJ, Baik J-J, Belcher SE, Beringer J, Bohnenstengel SI, Calmet I, Chen F, Coutts A, Dandou Fortuniak K, Gouvea ML, Hamdi R, Hendry M, Kanda M, Kawai T, Kawamoto Y, Kondo H, Krayenhoff ES, Lee S-H, Loridan T, Martilli A, Masson V, Miao S, Olsen K, Ooka R, Pigeon G, Porson A, Ryu Y-H, Salamanca F, Steeneveld GJ, Tombrou M, Voogt J, Young D, Zhang N. 2011. Initial results from phase 2 of the International Urban Energy Balance Model Comparison. *Int. J. Climatol.* **31**: 244−272, doi: 10.1002/joc.2227.

Hashimoto Y, Nabeshima M, Shigeta Y, Kikegawa Y, Ihara T. 2016. Analysis and discussion of sensitivity of electricity consumption to outdoor air temperature and air humidity in office and residential city blocks. *J. Environ. Eng.* **81**: 827−834, doi: 10.3130/aije.81.827. (in Japanese with English abstract).

Hong S -Y, Dudhia J, Chen S -H. 2004. A revised approach to ice microphysical processes for the bulk parameterization of clouds and precipitation. *Mon. Weather Rev.* **132**: 103−120, doi: 10.1175/1520-0493(2004)132<0103:ARATIM>2.0.CO;2.

Iacono MJ, Delamere JS, Mlawer EJ, Shephard MW, Clough SA, Collins WD. 2008. Radiative forcing by long−lived greenhouse gases: alculations with the AER radiative transfer models. *J. Geophys. Res.* **113**: D13103, doi: 10.1029/2008JD009944.

Ichinose T, Shimodozono K, Hanaki K. 1999. Impact of anthropogenic heat on urban climate in Tokyo. *Atmos. Environ.* **33**: 3897−3909, doi: 10.1016/S1352-2310(99)00132-6.

Ihara T, Genchi Y, Sato T, Yamaguchi K, Endo Y. 2008. City-block-scale sensitivity of electricity consumption to air temperature and air humidity in business districts of Tokyo, Japan. *Appl. Energy* **33**: 1634−1645, doi: 10.1016/j.energy.2008.06.005.

Iizuka S, Xuan Y, Kondo Y. 2015. Impacts of disaster mitigation/prevention urban structure models of future urban thermal environment. *Sustain. Cities Soc.* **19**: 414−420, doi: 10.1016/j.scs.2015.06.008.

IPCC. 2014. Summary for policymakers. In *Climate Change 2014: Impacts, Adaptation, and Vulnerability. Part A: Global and Sectoral Aspects. Contribution of Working Group II to the Fifth Assessment Report of the Intergovernmental Panel on Climate Change*, Field CB, Barros VR, Dokken DJ, Mach KJ, Mastrandrea MD, Bilir TE, Chatterjee M, Ebi KL, Estrada YO, Genova RC, Girma B, Kissel

ES, Levy AN, MacCracken S, Mastrandrea PR, White LL (eds). Cambridge University Press: Cambridge, UK; New York, NY, 1–32.
Janjic Z. 1994. The Step–Mountain Eta Coordinate Model: further developments of the convection, viscous sublayer, and turbulence closure schemes. *Mon. Weather Rev.* **122**: 927–945.
Janjic Z. 2002. Nonsingular implementation of the Mellor–Yamada level 2.5 scheme in the NCEP Meso model. NCEP Office Note 436, 61 pp.
Kalnay E, Kanamitsu M, Kistler R, Collins W, Deaven D, Gandin L, Iredell M, Saha S, White G, Woollen J, Zhu Y, Leetmaa A, Reynolds R. 1996. The NCEP/NCAR 40–year reanalysis project. *Bull. Am. Meteorol. Soc.* **77**: 437–471, doi: 10.1175/1520–0477(1996)077,0437:TNYRP.2.0.CO;2.
Kanda M, Inoue Y, Uno I. 2001. Numerical study on cloud lines over an urban street in Tokyo. *Bound.-Layer Meteorol.* **98**: 251–273, doi: 10.1023/A:1026504904902.
Kanda M, Kawai Y, Kanega M, Moriwaki R, Narita K, Hagishima A. 2005. A simple energy balance model for regular building arrays. *Bound.-Layer Meteorol.* **116**: 423–443, doi: 10.1007/s10546-004-7956-x.
Kikegawa Y, Genchi Y, Yoshikado Y, Kondo H. 2003. Development of a numerical simulation system for comprehensive assessments of urban warming countermeasures including their impacts upon the urban buildings' energy-demands. *Appl. Energy* **76**: 449–466, doi: 10.1016/S0306-2619(03)00009-6.
Kikegawa Y, Genchi Y, Kondo H, Hanaki K. 2006. Impacts of city-block-scale countermeasures against urban heat-island phenomena upon a building's energy-consumption for air-conditioning. *Appl. Energy* **83**: 649–668, doi: 10.1016/j.apenergy.2005.06.001.
Kikegawa Y, Tanaka A, Ohashi Y, Ihara T, Shigeta Y. 2014. Observed and simulated sensitivities of summertime urban surface air temperatures to anthropogenic heat in downtown areas of two Japanese Major Cities, Tokyo and Osaka. *Theor. Appl. Climatol.* **117**: 175–193, doi: 10.1007/s00704-013-0996-8.
Kikumoto H, Ooka R, Arima Y. 2016. A study of urban thermal environment in Tokyo in summer of the 2030s under influence of global warming. *Energy Build.* **114**: 54–61, doi: 10.1016/j.enbuild.2015.07.033.
Kimura F, Takahashi S. 1991. The effects of land–use and anthropogenic heating on the surface temperature in the Tokyo metropolitan area: a numerical experiment. *Atmos. Environ.* **25B**: 155–164, doi: 10.1016/0957-1272(91)90050-O.
Kondo H, Kikegawa Y. 2003. Temperature variation in the urban canopy with anthropogenic energy use. *Pure Appl. Geophys.* **160**: 317–324, doi: 10.1007/s00024-003-8780-9.
Kondo H, Liu FH. 1998. A study on the urban thermal environment obtained through a one-dimensional urban canopy model. *J.Jpn. Soc. Atmos. Environ.* **33**: 179–192. (in Japanese).
Kondo H, Genchi Y, Kikegawa Y, Ohashi Y, Yoshikado H, Komiyama H. 2005. Development of a multi-layer urban canopy model for the analysis of energy consumption in a big city: structure of the urban canopy model and its basic performance. *Bound.-Layer Meteorol.* **116**: 395–421, doi: 10.1007/s10546-005-0905-5.
Krpo A, Salamanca F, Martilli A, Clappier A. 2010. On the impact of anthropogenic heat fluxes on the urban boundary layer: a two-dimensional numerical study. *Bound.-Layer Meteorol.* **136**: 105–127, doi: 10.1007/s10546-010-9491-2.
Kurihara Y, Sakurai T, Kuragano T. 2006. Global daily sea surface temperature analysis using data from satellite microwave radiometer, satellite infrared radiometer and in-situ observation. *Weather Serv. Bull.* **73**: S1–S18. (in Japanese).
Kusaka H, Kimura F. 2004a. Coupling a single-layer urban canopy model with a simple atmospheric model: impact on urban heat island simulation for an idealized case. *J. Meteorol. Soc. Jpn.* **82**: 67–80, doi: 10.2151/jmsj.82.67.
Kusaka H, Kimura F. 2004b. Thermal effects of urban canyon structure on the nocturnal heat island: numerical experiment using a mesoscale model coupled with an urban canopy model. *J. Appl. Meteorol.* **43**: 1899–1910, doi: 10.1175/JAM2169.1.
Kusaka H, Kondo H, Kikegawa Y, Kimura F. 2001. A simple single–layer urban canopy model for atmospheric models: comparison with multi-layer and slab models. *Bound.-Layer Meteorol.* **101**: 329–358, doi: 10.1023/A:1019207923078.
Kusaka H, Takata T, Takane Y. 2010. Reproducibility of regional climate in central Japan using the 4-km resolution WRF model. *SOLA* **6**: 113–116, doi: 10.2151/sola.2010-029.
Kusaka H, Chen F, Tewari M, Dudhia J, Gill DO, Duda MG, Wang W, Miya Y. 2012a. Numerical simulation of urban heat island effects by the WRF model with 4-km grid increment: an inter-comparison study between the urban canopy model and slab model. *J. Meteorol. Soc. Jpn.* **90B**: 33–45, doi: 10.2151/jmsj.2012-B03.
Kusaka H, Hara M, Takane Y. 2012b. Urban climate projection by the WRF model at 3-km grid increment: dynamical downscaling and predicting heat stress in the 2070's August for Tokyo, Osaka, and Nagoya. *J. Meteorol. Soc. Jpn.* **90B**: 47–64, doi: 10.2151/jmsj.2012-B04.
Lemonsu A, Kounkou-Arnaud R, Desplat J, Salagnac J-L, Masson V. 2013. Evolution of the Parisian urban climate under a global changing climate. *Clim. Change* **116**: 679–692, doi: 10.1007/s10584-012-0521-6.
Martilli A, Clappier A, Rotach MW. 2002. An urban surface exchange parameterization for mesoscale models. *Bound.-Layer Meteorol.* **104**: 261–304, doi: 10.1023/A:1016099921195.
Masson V. 2000. A physically-based scheme for the urban energy budget in atmospheric models. *Bound.-Layer Meteorol.* **94**: 357–397, doi: 10.1023/A:1002463829265.
Masson V, Gomes L, Pigeon G, Liousse C, Pont V, Lagouarde J.-P, Voogt J, Salmond J, Oke TR, Hidalgo J, Legain D, Garrouste O, Lac C, Connan O, Briottet X, Lacherade S, Tulet P. 2008. The canopy and aerosol particles interactions in Toulouse urban layer (CAPITOUL) experiment. *Meteorog. Atmos. Phys.* **102**: 135–157, doi: 10.1007/s00703-008-0289-4.
Mellor GC, Yamada T. 1982. Development of a turbulence closure model for geophysical fluid problems. *Rev. Geophys. Space Phys.* **20**: 851–875, doi: 10.1029/RG020i004p00851.
Ministry of Economy, Trade and Industry of Japan. 2015. Energy white paper 2015. http://www.enecho.meti.go.jp/about/whitepaper/2015pdf/ (accessed 18 May 2016). (in Japanese).
Ohashi Y, Genchi Y, Kikegawa Y, Kondo H, Yoshikado H, Hirano Y. 2007. Influence of air-conditioning waste heat on air temperature in Tokyo office areas during summer: numerical experiments using an urban canopy model coupled with a building energy model. *J. Appl. Meteorol. Climatol.* **46**: 66–81, doi: 10.1175/JAM2441.1.
Ohashi Y, Kikegawa Y, Ihara T, Sugiyama N. 2014. Numerical simulations of outdoor heat stress index and heat disorder risk in the 23 wards of Tokyo. *J. Appl. Meteorol. Climatol.* **53**: 583–597, doi: 10.1175/JAMC-D-13-0127.1.
Ohashi Y, Ihara T, Kikegawa Y, Sugiyama N. 2016a. Numerical simulations of influence of heat island countermeasures on outdoor human heat stress in the 23 wards of Tokyo, Japan. *Energy Build.* **114**: 104–111, doi: 10.1016/j.enbuild.2015.06.027.
Ohashi Y, Suido M, Kikegawa Y, Ihara T, Shigeta Y, Nabeshima M. 2016b. Impact of seasonal variations in weekday electricity use on urban air temperature observed in Osaka, Japan. *Q. J. R. Meteorol. Soc.* **695**: 971–982, doi: 10.1002/qj.2698.
Osaka City. 2015. http://www.city.osaka.lg.jp/toshikeikaku/cmsfiles/contents/0000341/341575/1-3_siryo3.pdf (accessed 18 May 2016). (in Japanese).
Sailor DJ. 2011. A review of methods for estimating anthropogenic heat and moisture emissions in the urban environment. *Int. J. Climatol.* **31**: 189–199, doi: 10.1002/joc.2106.
Salamanca F, Martilli A. 2010. A new building energy model coupled with an urban canopy parameterization for urban climate simulations – part II. Validation with one dimension off-line simulations. *Theor. Appl. Climatol.* **99**: 345–356, doi: 10.1007/s00704-009-0143-8.
Salamanca F, Krpo A, Martilli A, Clappier A. 2010. A new building energy model coupled with an urban canopy parameterization for urban climate simulations – part I. Formulation, verification, and sensitivity analysis of the model. *Theor. Appl. Climatol.* **99**: 331–344, doi: 10.1007/s00704-009-0142-9.
Salamanca F, Georgescu M, Mahalov A, Moustaoui M, Wang M. 2013. Anthropogenic heating of the urban environment due to air conditioning. *J. Geophys. Res. Atmos.* **119**: 5949–5965, doi: 10.1088/1748-9326/8/3/034022.
Salamanca F, Georgescu M, Mahalov A, Moustaoui M, Wang M, Svoma BM. 2014. Assessing summertime urban air conditioning consumption in a semiarid environment. *Environ. Res. Lett.* **8**: 034022, doi: 10.1088/1748-9326/8/3/034022.
Seaman NL, Ludwig FL, Donall EG, Warner TT, Bhumralker CM. 1989. Numerical studies of urban planetary boundary-layer structure under realistic synoptic condition. *J. Appl. Meteorol.* **28**: 760–781, doi: 10.1175/1520-0450(1989)028<0760:NSOUPB>2.0.CO;2.
Shimoda Y, Takahara Y, Mizuno M. 2002. Estimation and impact assessment of energy flow in urban area. In *Proceedings of the 5th International Conference on EcoBalance*, S5–S28, 727–730.
Skamarock, WC, Klemp JB, Dudhia J, Gill DO, Barker DM, Duda MG, Huang X-Y, Wang W, Powers JG. 2008. A description of the Advanced Research WRF version 3. NCAR Technical Note NCAR/TN-4751STR, 113 pp. http://www.mmm.ucar.edu/wrf/users/docs/arw_v3.pdf. (accessed 18 May 2016).

Takane Y, Kusaka H. 2011. Formation mechanisms of the extreme high surface air temperature of 40.9°C observed in the Tokyo metropolitan area: considerations of dynamic foehn and foehn-like wind. *J. Appl. Meteorol. Climatol.* **50**: 1827–1841, doi: 10.1175/JAMC-D-10-05032.1.

Takane Y, Ohashi Y, Kusaka H, Shigeta Y, Kikegawa Y. 2013. Effects of synoptic-scale wind under the typical summer pressure pattern on the mesoscale high-temperature events in the Osaka and Kyoto urban areas by the WRF model. *J. Appl. Meteorol. Climatol.* **52**: 1764–1778, doi: 10.1175/JAMC-D-12-0116.1.

Takane Y, Aoki S, Kikegawa Y, Yamakawa Y, Hara M, Kondo H, Iizuka S. 2015a. Future projection of electricity demand and thermal comfort for August in Nagoya city by WRF–CM–BEM. *J. Environ. Eng.* **80**: 973–983, doi: 10.3130/aije.80.973. (in Japanese with English abstract).

Takane Y, Kusaka H, Kondo H. 2015b. Investigation of a recent extreme high-temperature event in the Tokyo metropolitan area using numerical simulations: The potential role of a 'hybrid' foehn wind. *Q. J. R. Meteorol. Soc.* **141**: 1857–1869, doi: 10.1002/qj.2490.

Tokairin T, Kondo H, Yoshikado H, Genchi Y, Ihara T, Kikegawa Y, Hirano Y, Asahi K. 2006. Numerical study on the effect of buildings on temperature variation in urban and suburban areas in Tokyo. *J. Meteorol. Soc. Jpn.* **84**: 921–937, doi: 10.2151/jmsj.84.921.

United Nations, Department of Economic and Social Affairs, Population Division. 2014. World urbanization prospects: the 2014 revision, highlights (ST/ESA/SER.A/352). https://esa.un.org/unpd/wup/publications/files/wup2014-highlights.Pdf (accessed 18 May 2016).

Yang L, Niyogi D, Tewari M, Aliaga D, Chen F, Tian F, Ni G. 2016. Contrasting impacts of urban forms on the future thermal environment: example of Beijing metropolitan area. *Environ. Res. Lett.* **11**: 034018, doi: 10.1088/1748-9326/11/3/034018.